Molecular Phylogenetics and Evolution 177 (2022) 107609

Contents lists available at ScienceDirect

Molecular Phylogenetics and Evolution

journal homepage: www.elsevier.com/locate/ympev

Phylogeny and evolution of morphological structures in a highly diverse lineage of fruiting-body-forming amoebae, order Trichiales (Myxomycetes, Amoebozoa)

Iván García-Cunchillos [a,*], Juan Carlos Zamora [b,c], Martin Ryberg [d], Carlos Lado [a]

[a] Real Jardín Botánico, CSIC, Plaza de Murillo 2, 28014 Madrid, Spain
[b] Conservatorie et Jardin Botaniques de la Ville de Genève, Chemin de l'Impératrice 1, 1292 Chambésy, Switzerland
[c] Museum of Evolution, Uppsala University, Norbyvägen 16, Uppsala 752 36, Sweden
[d] Department of Organismal Biology, Systematic Biology, Uppsala University, Norbyvägen 18D, Uppsala 752 36, Sweden

ARTICLE INFO

Keywords:
Ancestral state reconstructions
Evolution
Nomenclature
Phylogenetics
Systematics

ABSTRACT

Early phylogenetic studies refuted most previous assumptions concerning the evolution of the morphological traits in the fruiting bodies of the order Trichiales and did not detect discernible evolutionary patterns, yet they were based on a limited number of species. We infer a new Trichiales phylogeny based on three independently inherited genetic regions (nuclear and mitochondrial), with a fair taxonomic sampling encompassing its broad diversity. Besides, we study the evolutionary history of some key morphological characters. According to the new phylogeny, most fruiting body traits in Trichiales systematics do not represent exclusive synapomorphies or autapomorphies for most monophyletic groups. Instead, the evolution of the features derived from the peridium, stalk, capillitium, and spores showed intricate patterns, and character state transitions occurred rather within- than between clades. Thus, we should consider other evolutionary scenarios instead of assuming the homology of some characters. According to these results, we propose a new classification of Trichiales, including the creation of a new genus, *Gulielmina*, the resurrection of the family Dictydiaethaliaceae and the genus *Ophiotheca*, and the proposal of 13 new combinations for species of the genera *Arcyria* (1), *Hemitrichia* (2), *Ophiotheca* (2), *Oligonema* (4), *Gulielmina* (3), and *Perichaena* (1).

1. Introduction

The supergroup Amoebozoa comprises a highly diverse lineage of ameboid organisms with an exceptional variety of life cycles (Kang et al. 2017). Some amoebozoans can produce fruiting bodies in their life cycles, including the sorocarpic fruiting in dictyostelids (Schaap et al. 2006) and the formation of sporophores in Myxomycetes as well as the protosteloid amoebae (Adl et al. 2019). The latter evolved multiple times in Amoebozoa (Shadwick et al. 2009), and the last common ancestor to the supergroup may also have produced them (Kang et al. 2017). Thus, understanding the evolution of the morphological features in fruiting bodies of these lineages has become one of the main goals in systematics and evolutionary studies in Amoebozoa.

Fruiting bodies in Myxomycetes, more commonly referred to as sporophores (Fig. 1), contain the reproductive spores surrounded by an acellular envelope, the peridium, until their release. Sporophores anchor to the substrate by the hypothallus and can be either elevated by a stalk or be sessile. Besides, most species develop a capillitium, a system of sterile filaments intermingled with the spores. While the most common fruiting body morphology is the so-called sporocarp (Fig. 1), there are other three sporophores types: the plasmodiocarps, with elongated morphologies reminiscent of the plasmodium (one of the assimilative stages in Myxomycetes life cycle consisting of a naked, multinucleate mass of protoplasm), and two compound types, the pseudoaethalia and the aethalia (Keller et al. 2022). Despite this simplified definition, Myxomycetes fruiting bodies present highly variable colors, shapes, and sizes (see https://www.myxotropic.org/gallery/). Due to this diversity, Myxomycetes have a long-standing taxonomic tradition (Stephenson et al. 2008), and with 6–9 orders, 13–15 families, 68 genera (Lado and Eliasson 2022; Leontyev et al. 2019), and over 1,000 species (Lado 2005–2022) they are the lineage with more species recognized so far in Amoebozoa (Lara et al. 2020).

* Corresponding author.
E-mail address: igcun@rjb.csic.es (I. García-Cunchillos).

https://doi.org/10.1016/j.ympev.2022.107609
Received 29 March 2022; Received in revised form 14 June 2022; Accepted 5 August 2022
Available online 11 August 2022

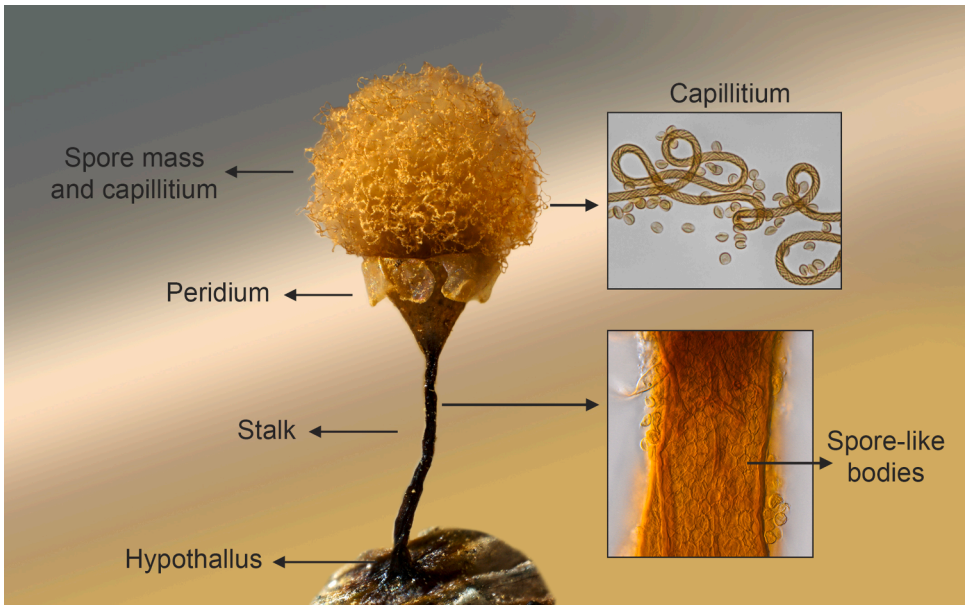

Fig. 1. General structure of a stalked sporocarp in Trichiales. The spores form a mass intermingled with the capillitium, a system of sterile filaments (up to the right, as seen with light microscopy), surrounded by a dehiscent peridium and anchored to the substrate by the hypothallus. This spore mass can be elevated above the substrate by a stalk or be sessile. In Trichiales, stalks can be filled with spore-like bodies (bottom right, as seen with light microscopy) or different refuse materials (not shown). Species: *Hemitrichia calyculata*.

Within this astonishing diversity, the order Trichiales T. Macbr. stands out as one of the most morphologically diverse orders, with nearly 200 species accepted (Lado 2005–2022). Trichiales are part of the Myxomycetes with bright-colored spores (Fiore-Donno et al. 2005) together with the orders Cribrariales T. Macbr., Reticulariales Leontyev, Schnittler, S.l. Stephenson, Novozhilov & Shchepin, and Liceales E. Jahn (Leontyev et al. 2019). Trichiales species develop unique elastic, thread-like, ornamented capillitium (Fig. 1). Instead, the capillitium is absent in Liceales and Cribrariales, while the species in Reticulariales produce pseudocapillitium, i.e., filiform peridium remnants (Lister 1925).

Despite the noticeable diversity, Trichiales systematics has remained stable over the years (e.g., Lister 1925; Martin and Alexopoulos 1969; Nannenga-Bremekamp 1991; Poulain et al. 2011; Rostafiński 1874, 1875, 1876). These taxonomic treatments assumed some evolutionary hypotheses concerning the capillitium to establish the Trichiales classification. Thus, the distinction between solid threads (family Dianemataceae) and hollow tubules (Arcyriaceae and Trichiaceae) defines the primary division. Differences between the latter two rely on the ornamental elements of the capillitium, consisting of spirals (Fig. 1) in the family Trichiaceae while being cogs, reticula, rings, spines, and verrucae in Arcyriaceae. Generic delimitation depends on other capillitium features, such as the branching pattern, or combinations of multiple macroscopic traits, like stalked vs. sessile sporocarps and evanescent vs. persistent peridium, distinguishing, for example, *Arcyria* from *Arcyodes* (Lado and Pando 1997). Some authors recognize a fourth monospecific family, Minakatellaceae, with unique pseudoaethaloid fruiting bodies in Trichiales, questioned by other authors (see Keller et al. 1973).

Unexpectedly, the introduction of DNA-based phylogenetic reconstructions in Trichiales (Fiore-Donno et al. 2013) has only confirmed some of the above-mentioned evolutionary hypotheses, while most of them have been refuted. For instance, the dichotomy between solid and hollow capillitium agrees with the phylogeny, although TEM-based studies reported at least four ultrastructural capillitium types of hollow filaments (Ellis et al. 1973; García-Cunchillos et al. 2021a). On the contrary, the spiral capillitium ornamentation seems to have originated independently in multiple clades (Fiore-Donno et al. 2013). Moreover, previous phylogenies recovered most genera in Trichiales as paraphyletic (Fiore-Donno et al. 2013; Leontyev et al. 2019; Ronikier et al.

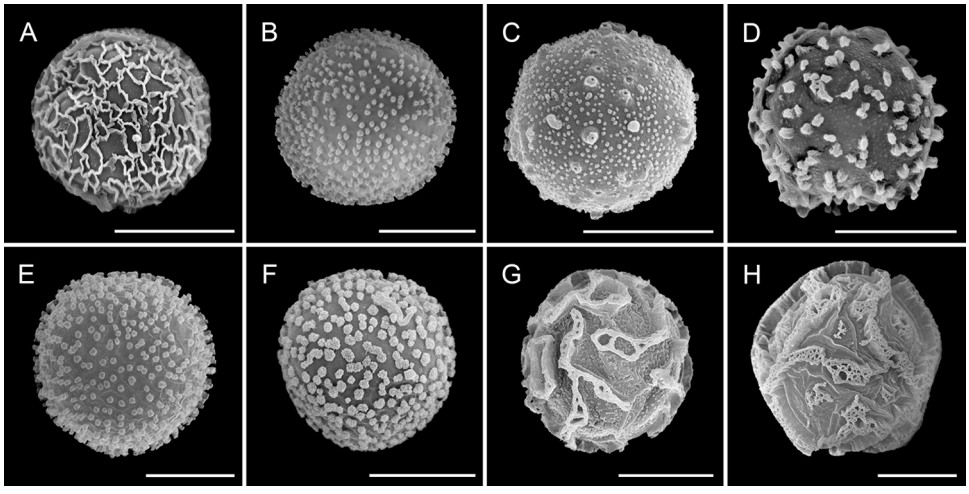

Fig. 2. Spore ornamentation types in Trichiales, as seen with scanning electron microscopy. **A** Simple reticulate (*Hemitrichia calyculata*). **B** Baculate (*Prototrichia metallica*). **C** Verrucate (*Arcyria denudata*). **D** Baculate (*Calonema foliicola*). **E** Baculate (*Perichaena quadrata*). **F** Pilate (*Metatrichia horrida*). **G** Cristate reticulate (*Hemitrichia serpula*). **H** Cristate patched (*Oligonema schweinitzii*). Scale bar = 5 μm.

Table 1
Species, specimens, and GenBank accession numbers of the sequences included in Trichiales phylogeny (Fig. 3). Taxonomy followed Lado and Eliasson (2022) and Leontyev et al. (2019). The nomenclatural treatment attended Lado (2005–2022). Species authorships can be consulted in Lado (2005–2022). The species name in bold indicates it as the type species of the genus. Accession numbers starting other than 'ON' correspond to the sequences retrieved from GenBank.

Order	Family	Species	Voucher	*18S rRNA*	*EF1A*	*mtSSU*
Liceales	Liceaceae	*Licea castanea*	AMFD 102	JX481295.1	JX481329.2	–
		Licea marginata	DWM 7368	JX481296.1	JX481330.1	–
		Licea parasitica	AMFD 341	JX481297.1	JX481331.1	–
Reticulariales	Reticulariaceae	***Lycogala epidendrum***	MA-Fungi 83194	ON713381.1	ON693913.1	ON713288.1
		Reticularia jurana	AMFD 290	JX481310.1	JX481339.1	–
		Reticularia jurana	MA-Fungi 83010	ON713377.1	–	ON713284.1
		Reticularia jurana	MA-Fungi 83011	ON713378.1	–	ON713285.1
		Reticularia jurana	MA-Fungi 83274	ON713384.1	–	ON713291.1
		Reticularia lycoperdon	AMFD 262	JX481311.1	JX481340.1	–
		Tubifera ferruginosa	AMFD 196	EF513171.1	EF513201.1	–
Trichiales	Arcyriaceae	***Arcyodes incarnata***	Lado 25434	ON713325.1	ON693868.1	ON713237.1
		Arcyodes incarnata	Lado 25437	ON713326.1	ON693869.1	ON713238.1
		Arcyria affinis	MA-Fungi 61187	ON713341.1	ON693881.1	ON713250.1
		Arcyria affinis	MA-Fungi 68912	ON713351.1	ON693886.1	ON713260.1
		Arcyria afroalpina	MA-Fungi 83613	ON713396.1	ON693927.1	ON713301.1
		Arcyria afroalpina	MA-Fungi 83614	ON713397.1	ON693928.1	ON713302.1
		Arcyria cinerea	MA-Fungi 83612	ON713395.1	ON693926.1	ON713300.1
		Arcyria cinerea	MA-Fungi 87452	ON713403.1	ON693934.1	ON713307.1
		Arcyria denudata	MA-Fungi 78718	ON713354.1	ON693889.1	–
		Arcyria denudata	MA-Fungi 83327	ON713385.1	ON693916.1	–
		Arcyria ferruginea	MA-Fungi 58962	ON713339.1	ON693879.1	ON713248.1
		Arcyria ferruginea	MA-Fungi 86476	ON713401.1	ON693932.1	ON713303.1
		Arcyria globosa	AMFD 252	JX481282.1	JX481318.1	–
		Arcyria globosa	MA-Fungi 52762	ON713335.1	–	ON713244.1
		Arcyria incarnata	MA-Fungi 83426	ON713390.1	ON693921.1	ON713295.1
		Arcyria incarnata	MA-Fungi 83465	ON713392.1	ON693923.1	ON713297.1
		Arcyria insignis	MA-Fungi 87847	ON713404.1	ON693935.1	ON713308.1
		Arcyria insignis	MA-Fungi 87859	ON713405.1	ON693936.1	ON713309.1
		Arcyria oerstedii	MA-Fungi 58741	ON713337.1	ON693877.1	ON713246.1
		Arcyria oerstedii	MA-Fungi 61817	ON713342.1	ON693882.1	ON713251.1
		Arcyria stipata	AMFD 257	EF513170.1	EF513183.1	–
		Cornuvia serpula	MM 29198	JX481285.1	JX481320.1	–
		Perichaena calongei	Lado 25554	ON713327.1	ON693870.1	ON713239.1
		Perichaena calongei	MA-Fungi 78686	ON713352.1	ON693887.1	ON713261.1
		Perichaena calongei	MA-Fungi 78692	ON713353.1	ON693888.1	ON713262.1
		Perichaena chrysosperma	MA-Fungi 63754	ON713345.1	ON693883.1	ON713254.1
		Perichaena chrysosperma	MA-Fungi 64647	ON713349.1	–	ON713258.1
		Perichaena corticalis	MA-Fungi 68850	ON713350.1	ON693885.1	ON713259.1
		Perichaena corticalis	MA-Fungi 83138	ON713380.1	ON693912.1	ON713287.1
		Perichaena depressa	MA-Fungi 83635	ON713398.1	ON693929.1	–
		Perichaena depressa	MA-Fungi 88312	ON713408.1	ON693939.1	–
		Perichaena dictyonema	MA-Fungi 59057	ON713340.1	ON693880.1	ON713249.1
		Perichaena liceoides	M 0073211	ON713328.1	ON693871.1	–
		Perichaena liceoides	M 0073215	ON713329.1	ON693872.1	–
		Perichaena megaspora	KRAM-M 1765	MT154023.1	MT162162.1	–
		Perichaena megaspora	MA-Fungi 82123	MT154026.2	MT162165.1	ON713281.1
		Perichaena nigra	MA-Fungi 86774	ON713402.1	ON693933.1	ON713306.1
		Perichaena patagonica	MA-Fungi 91906	MT154034.2	MT162173.1	ON713317.1
		Perichaena patagonica	MA-Fungi 91909	MT154035.2	MT162174.1	ON713318.1
		Perichaena pedata	MA-Fungi 81941	ON713372.1	ON693906.1	ON713280.1
		Perichaena quadrata	MA-Fungi 88308	ON713406.1	ON693937.1	ON713310.1
		Perichaena quadrata	MA-Fungi 88310	ON713407.1	ON693938.1	ON713311.1
		Perichaena stipitata	MA-Fungi 79150	ON713358.1	ON693892.1	ON713265.1
		Perichaena stipitata	MA-Fungi 79151	ON713359.1	ON693893.1	ON713266.1
		Perichaena vermicularis	BR 5020025765604	MT154019.1	MT162157.1	–
		Perichaena vermicularis	MA-Fungi 80426	ON713363.1	ON693897.1	ON713270.1
		Perichaena vermicularis	MA-Fungi 88424	ON713409.1	–	ON713313.1
	Dianemataceae	***Calomyxa metallica***	AMFD 483	JX481284.1	JX481319.1	–
		Calomyxa metallica	IT 560	ON713323.1	ON693865.1	ON713234.1
		Calomyxa metallica	MA-Fungi 82936	ON713373.1	ON693907.1	–
		Calomyxa metallica	MA-Fungi 82941	ON713375.1	ON693909.1	ON713283.1
		Calomyxa metallica	MA-Fungi 82942	ON713376.1	ON693910.1	–
		Dianema corticatum	KR-M 0040806	MT154024.1	MT162163.1	–
		Dianema corticatum	KR-M 0040819	MT154025.1	MT162164.1	–
		Dianema depressum	MA-Fungi 80673	ON713367.1	ON693900.1	ON713273.1
		Dianema depressum	MA-Fungi 82939	ON713374.1	ON693908.1	ON713282.1
		Dianema harveyi	BR 5020022218059	MT154018.1	MT162156.1	–
		Dianema harveyi	BR 5020210944555V	MT154020.1	MT162158.1	–
		Dianema inconspicuum	MM 39161	MT154038.2	MT162177.1	ON713320.1
		Dianema mongolicum	MM 45002	ON713413.1	ON693944.1	ON713321.1

(*continued on next page*)

Table 1 (*continued*)

Order	Family	Species	Voucher	*18S rRNA*	*EF1A*	*mtSSU*
		Dianema nivale	MM 29888	JX481289.1	JX481324.1	–
		Dianema sp.	MA-Fungi 86506	MT154027.2	MT162166.1	ON713304.1
		Dianema sp.	MA-Fungi 86507	MT154028.2	MT162167.1	ON713305.1
		Dianema subretisporum	MM 31413	ON713412.1	ON693943.1	ON713319.1
		Dianema subretisporum	MM 46699	ON713414.1	ON693945.1	ON713322.1
		Dianema succulenticola	MA-Fungi 80774	–	ON693901.1	ON713274.1
		Dianema succulenticola	MA-Fungi 81387	–	ON693903.1	ON713276.1
		Dictydiaethalium dictyosporum	MA-Fungi 91171	ON713411.1	ON693942.1	ON713314.1
		Dictydiaethalium plumbeum	MA-Fungi 64421	ON713348.1	ON693884.1	ON713257.1
		Licea variabilis	MA-Fungi 80591	ON713366.1	ON693899.1	ON713272.1
		Licea variabilis	MA-Fungi 85637	ON713400.1	ON693931.1	–
		Prototrichia metallica	MA-Fungi 80049	ON713360.1	ON693894.1	ON713267.1
		Prototrichia metallica	MM 24907	JX481309.1	JX481338.1	–
	Trichiaceae	*Calonema foliicola*	MA-Fungi 50720	ON713333.1	ON693875.1	–
		Hemitrichia abietina	MA-Fungi 58838	ON713338.1	ON693878.1	ON713247.1
		Hemitrichia abietina	MM 30370	JX481293.1	JX481327.1	–
		Hemitrichia calyculata	MA-Fungi 81807	ON713370.1	–	ON713278.1
		Hemitrichia calyculata	MS 22060	JX481294.1	JX481328.1	–
		Hemitrichia clavata	MA-Fungi 62017	ON713343.1	–	ON713252.1
		Hemitrichia clavata	MA-Fungi 62018	ON713344.1	–	ON713253.1
		Hemitrichia crassifila	MA-Fungi 91880	MT154030.2	MT162169.1	ON713315.1
		Hemitrichia crassifila	MA-Fungi 91885	MT154031.2	MT162170.1	ON713316.1
		Hemitrichia intorta	BR 5020003245449	MT154017.1	MT162155.1	–
		Hemitrichia intorta	KR 0022295	MT154021.1	MT162159.1	–
		Hemitrichia leiocarpa	M 0142937	ON713330.1	–	ON713240.1
		Hemitrichia minor	MA-Fungi 80197	ON713361.1	ON693895.1	ON713268.1
		Hemitrichia minor	U 6369	ON713415.1	ON693946.1	–
		Hemitrichia pardina	MA-Fungi 80413	ON713362.1	ON693896.1	ON713269.1
		Hemitrichia serpula	MA-Fungi 64060	ON713346.1	–	ON713255.1
		Hemitrichia serpula	MA-Fungi 64068	ON713347.1	–	ON713256.1
		Metatrichia floriformis	MA-Fungi 52989	ON713336.1	–	ON713245.1
		Metatrichia floriformis	MA-Fungi 83204	ON713382.1	ON693914.1	ON713289.1
		Metatrichia floripara	Lado 25103	ON713324.1	ON693867.1	ON713236.1
		Metatrichia horrida	MA-Fungi 81778	ON713369.1	ON693904.1	ON713277.1
		Metatrichia horrida	MA-Fungi 81857	ON713371.1	ON693905.1	ON713279.1
		Metatrichia vesparia	MA-Fungi 51719	ON713334.1	ON693876.1	ON713243.1
		Metatrichia vesparia	MA-Fungi 88351	–	ON693940.1	ON713312.1
		Oligonema schweinitzii	MA-Fungi 85559	ON713399.1	ON693930.1	–
		Oligonema schweinitzii	MM 29842	JX481305.1	JX481336.1	–
		Oligonema sp.	MA-Fungi 78856	ON713355.1	ON693890.1	–
		Oligonema sp.	MA-Fungi 78857	ON713356.1	ON693891.1	ON713263.1
		Oligonema sp.	MA-Fungi 83328	ON713386.1	ON693917.1	ON713292.1
		Oligonema sp.	MA-Fungi 83357	ON713389.1	ON693920.1	ON713294.1
		Trichia affinis	Lado 24817	–	ON693866.1	ON713235.1
		Trichia affinis	MA-Fungi 78975	ON713357.1	–	ON713264.1
		Trichia affinis	MA-Fungi 83345	ON713387.1	ON693918.1	–
		Trichia agaves	MA-Fungi 42243	ON713331.1	ON693873.1	ON713241.1
		Trichia agaves	MA-Fungi 50703	ON713332.1	ON693874.1	ON713242.1
		Trichia alpina	AMFD 64	JX481312.1	JX481341.1	–
		Trichia alpina	MA-Fungi 80534	ON713364.1	–	ON713271.1
		Trichia decipiens	MA-Fungi 83070	ON713379.1	ON693911.1	ON713286.1
		Trichia favoginea	MA-Fungi 83229	ON713383.1	ON693915.1	ON713290.1
		Trichia lutescens	MA-Fungi 83355	ON713388.1	ON693919.1	ON713293.1
		Trichia lutescens	MA-Fungi 83430	ON713391.1	ON693922.1	ON713296.1
		Trichia persimilis	–	AY643826.1	AY643821.1	–
		Trichia scabra	MA-Fungi 81001	ON713368.1	ON693902.1	ON713275.1
		Trichia scabra	MA-Fungi 90224	ON713410.1	ON693941.1	–
		Trichia scabra	MS 22055	JX481314.1	JX481343.1	–
		Trichia sordida	AMFD 81	EF513182.1	EF513200.1	–
		Trichia varia	MA-Fungi 80566	ON713365.1	ON693898.1	–
		Trichia varia	MA-Fungi 83469	ON713393.1	ON693924.1	ON713298.1
		Trichia verrucosa	MA-Fungi 83489	ON713394.1	ON693925.1	ON713299.1

2020; Walker et al. 2015).

Consequently, it is necessary to investigate other characters previously overlooked to test whether they reflect evolutionary relationships. For example, Fiore-Donno et al. (2013) proposed the spore-like bodies, structures filling the stalks in certain species (Fig. 1), as a diagnostic character of a clade comprising some species of the genera *Trichia* and *Hemitrichia*. Other features, traditionally considered variable, such as the spore ornamentation (Fig. 2), could show more straightforward patterns of evolution (García-Cunchillos et al. 2021b). However, there is still an underrepresentation of Trichiales diversity in phylogenetic studies to understand the evolutionary histories of many morphological characters.

In this study, we infer a new Trichiales phylogeny with a representative sampling of the morphological diversity encompassed in the order. In this new framework, we trace the evolutionary patterns of the principal morphological features of fruiting bodies, such as the distinct capillitium traits or sporophore types. In particular, we focus on four characters: stalks, spore-like bodies, number of peridium layers, and spore ornamental elements, for which we also conduct, for the first time in Myxomycetes, ancestral state reconstructions to explore and unravel the evolutionary

history of these characters. Lastly, we provide a revised systematic classification of the major groups in Trichiales by proposing taxonomic amendments for some taxa to reflect both the phylogenetic affinities and the evolution of the morphological traits.

2. Material and methods

2.1. Samples

We obtained new genetic information from three families, 13 genera, and 61 species of Trichiales, plus two genera and two species of Reticulariales as part of the phylogeny outgroup (Supplementary material 1). Whenever possible, we selected two specimens of each species and performed independent DNA extraction shifts to ensure the identity of the new sequences. We further completed the sampling with GenBank public data, with species that available *18S rRNA* and *EF1A* sequences belong to the same voucher (grey-shaded in Table 1), including representatives from the orders Reticulariales and Liceales. The final dataset comprised representatives of almost all families, 73 species, and 132 specimens (Table 1). Besides, we studied 57 samples of 32 species for which DNA obtaining failed; we provide this information since it may be informative for future studies dealing with these species (Supplementary material 2). Unfortunately, we could not obtain specimens of *Minakatella longifila*, the monospecific genus of the family Minakatellaceae.

Different phylogenetic and morphological studies detected striking contrasts when comparing specimens of a presumably single species from the northern and southern hemispheres (Janik et al. 2020, 2021; Ronikier and Lado 2015), particularly between the Neotropics and Europe, the latter often being the origin for the descriptions of multiple species. However, the European specimens we could study were, in most cases, aged, and we could not obtain enough genetic information. To palliate this shortcoming, we have alternatively constructed an *18S rRNA*-based phylogeny including all *18S rRNA* sequences analyzed in our multilocus phylogeny (Table 1) plus other available sequences in GenBank of the same studied species but from different geographic origins (Supplementary material 3). Our objective with this *18S rRNA*-based phylogeny was to confirm that samples of presumably single species but from distant geographical regions were at least nesting in the same principal clades, and then our diagnoses of these groups and nomenclatural changes were not compromised by sampling bias.

Taxonomy followed Leontyev et al. (2019) and Lado and Eliasson (2022). The nomenclatural treatment attended Lado (2005–2022). Vouchers of all specimens studied came from the herbaria BR, KR-M, KRAM-M, M, MA-Fungi (https://sweetgum.nybg.org/science/ih/), and private collections of I. Treviño-Zevallos, C. Lado, M. Meyer, and U. Eliasson.

2.2. DNA Extraction, PCR Amplification, and sequencing

Four to eight adjacent sporocarps, or an equivalent portion in plasmodiocarpic and pseudoaethaloid specimens, were selected for total DNA extraction. Each sample was transferred to a safe-lock microcentrifuge tube containing one 3 mm diam. tungsten carbide bead, frozen at −80 °C for one hour, and then subjected to mechanical disruption in a TissueLyser II bead mill, according to Fiore-Donno et al. (2012). DNA extraction followed the DNeasy Plant Mini Kit (QIAGEN, Germany) protocol with two minor modifications: i) samples were incubated in the buffer AP1 overnight, and ii) DNA was eluted twice with 80 μL of the buffer AE.

To infer the new Trichiales phylogeny, we selected two nuclear (the nuclear small subunit ribosomal RNA or *18S rRNA* and the eukaryotic translation elongation factor 1 alpha or *EF1A*) and one mitochondrial (the mitochondrial small subunit ribosomal RNA or *mtSSU*) genetic regions. Among the former, the *18S rRNA* is the preferred region to study phylogenetic relationships within Myxomycetes (see Schnittler et al. 2017), which, combined with the *EF1A*, recovered statistically supported clades at various taxonomic ranks (e.g., Fiore-Donno et al. 2005, 2012, 2013, 2018). The *mtSSU* reported coherent results compared to other genetic regions in the dark-spored Myxomycetes (Lado et al. 2022), but no studies have explored this region in the bright-spored Myxomycetes with phylogenetic purposes.

The *18S rRNA* sequence length varied 1387–2515 bp due to the presence of introns and the highly variable helices (Fiore-Donno et al. 2012). Consequently, it was amplified and sequenced in three fragments: S1 (509–786 bp), S2 (790–1601 bp), and S3 (707–1279 bp). To apply this so-called primer walking method (Fraser and Fleischmann 1997), the end of each fragment must partially overlap with the beginning of the next one: S1–S2 (187–203 bp overlapping) and S2–S3 (246–249 bp). When S2 or S3 amplifications failed, we completed these positions as Ns (any base) in the alignment, treated as missing data in subsequent analyses. For the amplification of the first fragment (S1), we employed primers SF01, SF02*, and SR01 (Ronikier et al. 2020), in which F and R refer to forward and reverse, respectively, and an asterisk (*) designates its use as inner forward primer in semi-nested PCRs. Following the same nomenclature, we designed new primers (sequences in 5′ → 3′ direction) to amplify fragments S2 (SF03: ACGGGTACAGAGGATCAG; SF04*: AGCCTGAGAGATCGCTAC, and SR02: CCTTGTGTGCTCTTCCGT) and S3 (SF05: TAGGGGTGAAATCCGTTGA, SF06*: ACGAAAGTCTGGGGAT, and SR3: TACAAAGAGCAGGGACA). The *EF1A* was amplified and sequenced as a single amplicon, including the intron present in every Myxomycetes species (Fiore-Donno et al. 2005), and sequences ranged from 876 to 1453 bp. Forward primers for *EF1A* amplification were EF03 and EF04* (Ronikier et al. 2020), and the reverse primer was KEF_R3 (García-Martín et al. 2018). The *mtSSU* sequences comprised 334–667 bp, amplified as a single amplicon with the primers pair Kmit_F and Kmit_R (Lado et al. 2022). We did not obtain successful amplification by using inner primers in semi-nested PCRs.

Each PCR reaction contained 12.5 μL MyTaq^{TM} DNA Polymerase (BIOLINE, United Kingdom), 1 μL DMSO, 0.5 μL of each primer, forward and reverse (10 mM), 1–3 μL template DNA, and completed with Milli-Q water up to a final volume of 25 μL. Semi-nested PCRs used 1 μL of a dilution 1:10 of the original PCR product. PCR conditions for the amplification of each genetic region included an initial denaturation step (94 °C, 1 min), 30 cycles consisting of denaturation (94 °C, 1 min), annealing (50–52 °C according to each primer, 1 min), and extension (72 °C, 3 min), and a final extension step (72 °C, 10 min). Successful amplifications were checked through electrophoresis in 1 % agarose gels and 1 × TAE buffer and purified with the QIAquick Gel Extraction Kit (QIAGEN, Germany). Amplicons were sequenced in both directions, with the same primer pairs, at MACROGEN facilities in Madrid (Spain).

2.3. Alignments

The newly obtained sequences, along with those retrieved from GenBank, were aligned for each genetic region with the MAFFT online service (https://mafft.cbrc.jp/alignment/server/) of MAFFT 7 (Katoh et al. 2019), using the L-INS-i strategy (Katoh et al. 2005), and the remaining parameters as default. Every alignment was visually inspected and manually corrected when detecting errors. We discarded introns in the *EF1A* alignment (positions 226–4708, Supplementary material 4) for further analyses since they were highly divergent to be consistently aligned. Thus, the *EF1A* dataset consisted of 117 sequences and 1017 bp. Similarly, barely alignable positions in the *mtSSU* alignment were discarded (289–4004, Supplementary material 5), and the dataset comprised 89 sequences and 375 bp.

Highly divergent intron sequences and variable helices of the *18S rRNA* resulted in multiple poorly aligned positions. Thus, a mask based on predicted secondary structures of rRNA in the bright-spored Myxomycetes was employed (Fiore-Donno et al. 2013), retaining only those positions under the mask (Supplementary material 6). The new *18S rRNA* sequences were added to an existing masked alignment (Fiore-Donno et al. 2013), including some of the sequences obtained from

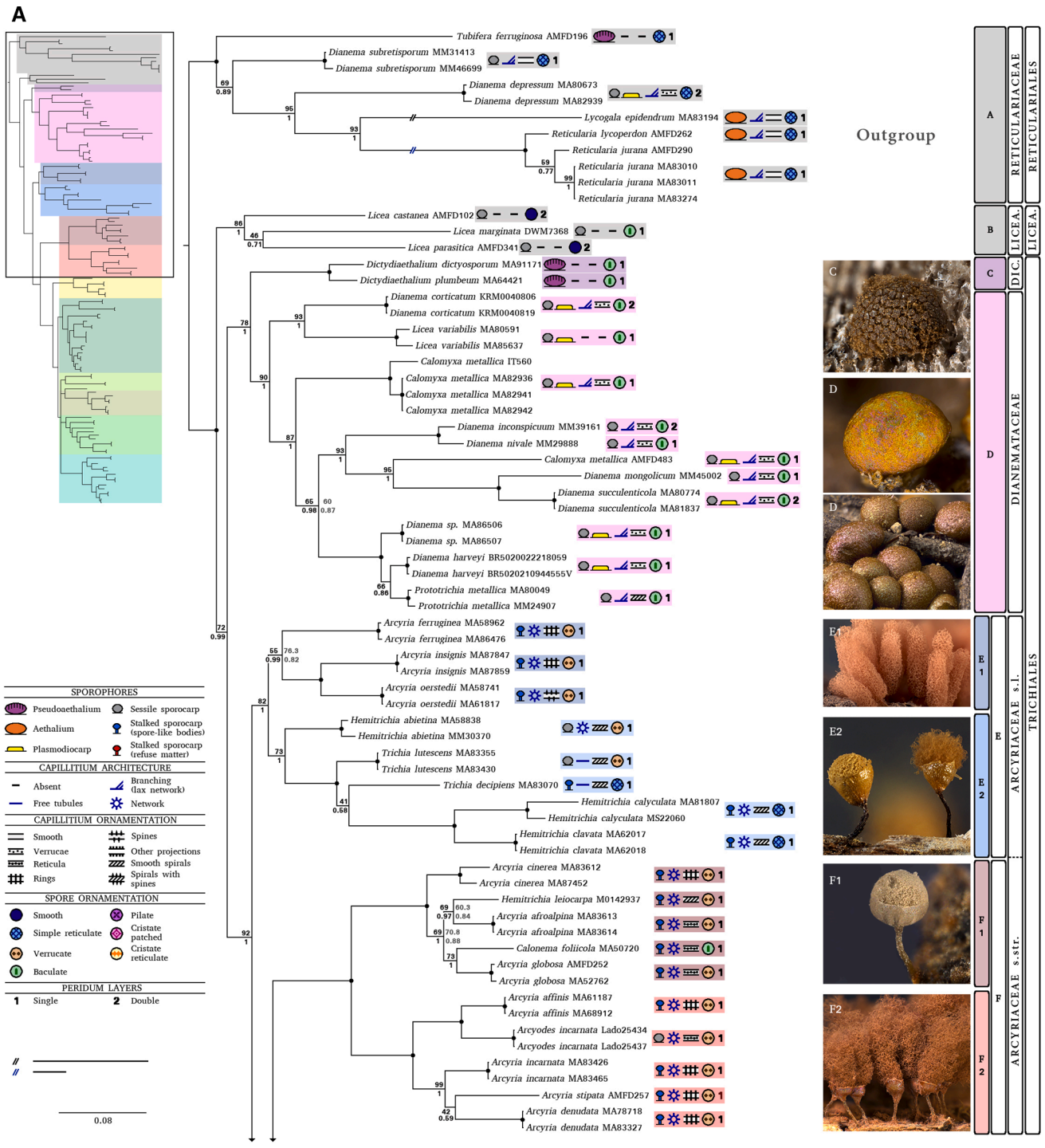

Fig. 3. Phylogeny of the order Trichiales based on 132 specimens and 73 species (Table 1), including Reticulariales and Liceales as the outgroup. Majority-rule consensus Bayesian tree obtained from the concatenated genetic regions *18S rRNA* (1246 bp), *EF1A* (1017 bp), and *mtSSU* (375 bp). Phylogenetic supports include Felsenstein's Bootstrap Proportions and Bayesian Posterior Probabilities, above and below each branch, respectively. Full phylogenetic support, i.e., Felsenstein's Bootstrap Proportions = 100 and Bayesian Posterior Probabilities = 1, is represented by a black circle. SH-aLRT and Transfer Bootstrap Expectation are only provided (in grey to the right of the previous ones, above and below, respectively) when the former support values recovered conflictive results. The scale bar indicates the average number of substitutions per site. Double slashes indicate shortened branches. To the right of vouchers, representation of the principal studied morphological features are depicted (see legend): fruiting body types, capillitium architecture, capillitium ornamentation (simplified), spore ornamentation, and peridium number of layers. **C** *Dictydiaethalium plumbeum*. **D** *Calomyxa metallica* (above), *Dianema harveyi* (below). **E1** *Arcyria insignis*. **E2** *Hemitrichia calyculata*. **F1** *Arcyria globosa*. **F2** *Arcyria affinis*. **G** *Perichaena calongei*. **H1** *Hemitrichia serpula* (above), *Trichia affinis* (middle), *Trichia verrucosa* (below). **OT** *Trichia varia*. **H2** *Perichaena patagonica*. **H3** *Metatrichia floriformis*. **H4** *Perichaena stipitata* (above), *Perichaena depressa* (below).

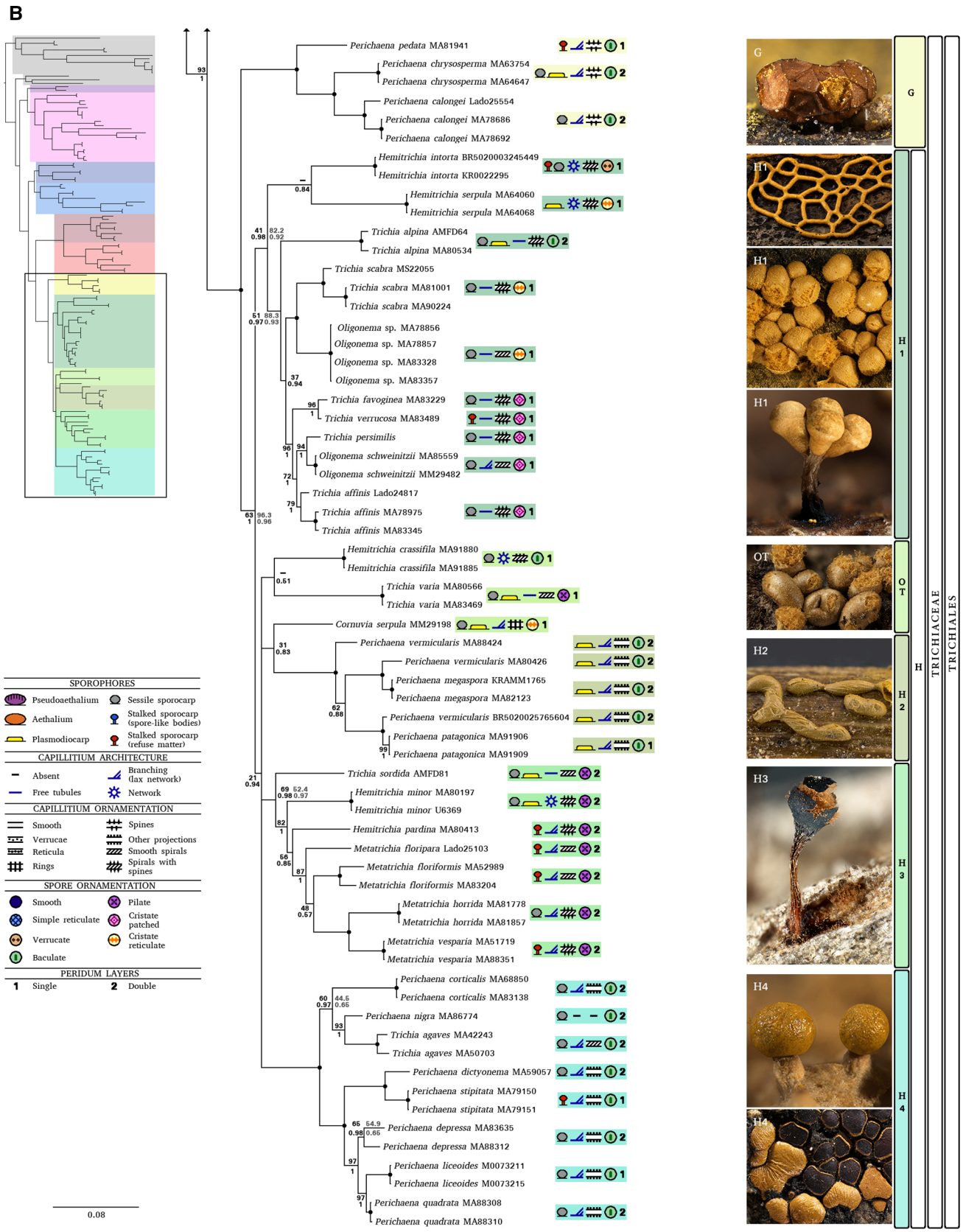

Fig. 3. (*continued*).

Genbank, using the option –add of MAFFT (Katoh and Frith 2012). The final *18S rRNA* dataset comprised 128 sequences and 1246 bp. Since we did not detect supported incongruences among the phylogenies inferred from these datasets, a fourth dataset was constructed by concatenating the individual alignments. Missing data in this dataset consisted of Ns. Gaps were treated as missing data in the subsequent analyses.

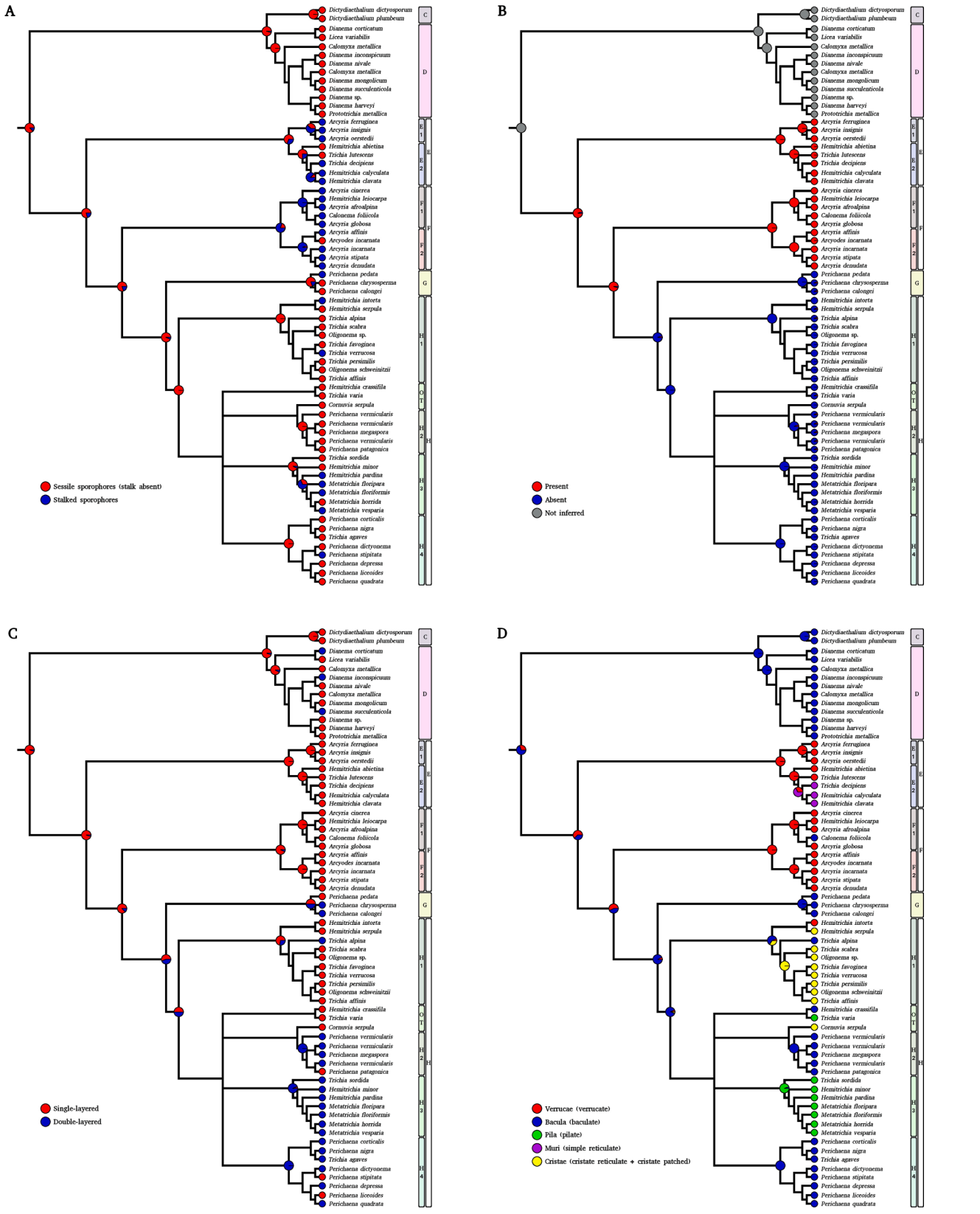

Fig. 4. Ancestral state reconstructions for selected characters based on stochastic character mapping simulations. Clade names (to the right of each cladogram) matched those in Fig. 3. **A** Stalk (red = absent, blue = present). **B** Spore-like bodies (red = present, blue = absent). Clades C and D were excluded from the analysis (see Material and Methods), and the involved nodes were not inferred (grey circles). **C** Number of peridium layers (red = single-layered, blue = double-layered). **D** Spore-ornamental elements (red = verrucae, blue = bacula, green = pila, purple = muri, cristae = yellow), in parentheses, corresponding ornamentation types. (For interpretation of the references to color in this figure legend, the reader is referred to the web version of this article.)

2.4. Phylogenetic analyses

Maximum likelihood trees were inferred with IQ-TREE 2.0 (Nguyen et al. 2015). The best-fit substitution model for each dataset was selected with ModelFinder (Kalyaanamoorthy et al. 2017) under the Bayesian information criterion (BIC). The concatenated dataset consisted of five partitions: *18S rRNA*, *mtSSU*, and three blocks of the *EF1A* corresponding to the first, second, and third codon positions. For each dataset or partition, model parameters were estimated with edge-linked branch lengths, and the best partition scheme was selected using the greedy search algorithm as implemented in IQ-TREE 2.0 (Chernomor et al. 2016). We conducted ten independent runs for the analyses of each dataset, including the concatenated one, as recommended by Zhou et al. (2018). To further minimize the possibility that the tree search algorithms could get stuck in local optima, we set a smaller value of the parameter perturbation strength for randomized NNI (-pers 0.2) and a higher number of unsuccessful iterations to stop (-nstop 500), as recommended in Nguyen et al. (2015).

Phylogenetic trees were also inferred under a Bayesian approach using MRBAYES 3.2.7a (Ronquist et al. 2012) with the parallel Metropolis-coupled Markov chain Monte Carlo ($[MC]^3$) algorithm (Altekar et al. 2004). The same partition blocks as in the maximum likelihood analyses were defined, with unlinked parameters estimation but linked tree topologies. The estimation of DNA models of evolution employed the Reversible Jump Markov Monte Carlo method (Huelsenbeck et al. 2004). Markov chain Monte Carlo (MCMC) simulations consisted of four runs, four chains each, and 20,000,000 generations. Trees were sampled every 1,000 generations, with a 0.25 fraction of the samples discarded as burn-in. Diagnosis of convergence was assessed through the average standard deviation of split frequencies (ASDSF, ideally ≤ 0.01), the potential scale reduction factors (PSRF ≈ 1.000), and the inspection of the Effective Sample Sizes (ESS ≥ 200) of each sampled parameter through TRACER 1.7.1 (Rambaut et al. 2018).

Branch phylogenetic supports were assessed with the two most broadly employed methods in phylogenetic studies (Wróbel 2008), i.e., the Felsenstein's bootstrap proportions (FBP) and the Bayesian Posterior Probabilities (BPP). The former was estimated with 1,000 nonparametric replicates in IQ-TREE 2.0 (Chernomor et al. 2016), and the latter in MRBAYES 3.2.7a (Ronquist et al. 2012) after discarding the 0.25 fraction of the sampled trees. While both methods usually agreed in detecting supported (i.e., FBP ≥ 70 and BPP ≥ 0.95) and unsupported clades, they recovered conflicting results for some of them. As recommended in Wróbel (2008), we estimated a third, approximate likelihood-based measure of branch supports, the SH-aLRT (Anisimova et al. 2011; Guindon et al. 2010), in IQ-TREE 2.0 with 1,000 nonparametric replicates (supported clades when SH-aLRT $\geq$ 80). Besides, Lemoine et al. (2018) proposed a modification of the FBP, the transfer bootstrap expectation (TBE), considering the effect of rogue taxa in molecular phylogenies, usually decreasing FBP values. TBE relied on the same 1,000 nonparametric replicates as FBP estimation and were estimated in the online service BOOSTER (https://booster.pasteur.fr/). Clades were considered supported when TBE ≥ 0.80.

2.5. Character evolution analyses

We reconstructed the character state at ancestral nodes for the following traits: stalk (absent, present), spore-like bodies (present, absent), the number of perdium layers (single-layered, double-layered), and spore ornamental elements (muri, bacula, verrucae, pila, and cristae). Each ornamental element defines a spore ornamentation type (Rammeloo 1974): simple reticulate (muri, strip-like elements with smooth tops, Fig. 2A), baculate (bacula, cylindrical, taller than broad elements with rounded or short-pointed tops, Fig. 2B, D–E), verrucate (verrucae, rounded, broader than tall elements, Fig. 2C), pilate (pila, cylindrical elements supporting spherical head-like structures, Fig. 2F), and cristate (cristae, elements similar to muri but with irregularly shaped tops, Fig. 2 G–H). Cristate ornamentation encompasses two subtypes (see García-Cunchillos et al. 2021b), the cristate reticulate (Fig. 2G) and the cristate patched (Fig. 2H). While, for more detailed information, we refer to both subtypes in the mapping of characters (Fig. 3) and the discussion, we do not consider this distinction in the ancestral state reconstructions (Fig. 4) since the ornamental element is the same, and, in this way, we also minimize the total number of possible states for the ancestral state reconstruction analyses. For the species producing sessile sporophores, the character "spore-like bodies" is unknown, so we established prior probabilities equally divided among all possible states, following Zamora and Ekman (2020). Besides, for this character, we ran the analyses twice: first, considering all the clades, and second, excluding clades C and D, in which states in all taxa are unknown since all species lack stalks (see Results).

The reconstructions started from a random sample of 1,000 trees (phylograms) from the total Bayesian posterior tree sampling. Phylograms were pruned to conserve one specimen per species (the one with the shortest branch) and exclude the outgroup. Ancestral state reconstructions relied on stochastic character mappings, performed with SIMMAP (Bollback 2006), using the *make.simmap()* function implemented in the R package phytools (Revell 2012). Analyses consisted of ten character mapping simulations for each phylogram (Zamora and Ekman 2020). We set an asymmetric model for characters with only two states and a symmetric model for characters with more than two states (see Kistenich et al. 2018).

Ancestral state reconstructions based on phylograms (i.e., considering morphological change proportional to genetic change) and chronograms (i.e., morphological change proportional to time) may yield different results (Cusimano and Renner 2014; Litsios and Salamin 2012). Thus, we also conducted the same analyses starting from chronograms. Chronograms were generated from the phylograms with the function *chronos()* implemented in the R package ape v.5.0 (Paradis and Schliep 2019), which uses penalized likelihoods under a correlated model as described by Paradis (2013). Here, both versions of the analyses (phylograms vs. chronograms) reported slightly different results. However, the differences occurred at nodes for which none of the analyses reported conclusive results. Thus, we only show the results of the reconstructions based on phylograms.

3. Results

3.1. Phylogeny of the order trichiales

The ten maximum-likelihood tree searches resulted in highly similar log-likelihood scores, with only marginal differences, for all datasets (results not shown). Nonetheless, we selected the trees with the highest score for further study. The best partition scheme in the *EF1A* genetic region consisted of three blocks, one for each position in the codon-triplets. The best-fitting substitution models for these blocks were TIM3 + I + G, GTR + I + G, and GTR + G, respectively. *EF1A* was the least informative region and only supported phylogenetic affinities among specimens of the same species or closely related taxa, while the remaining clades received negligible support. The *18S rRNA* and the *mtSSU* regions were comparatively more informative, and both reported highly similar topologies. The best-fitting substitution models for these regions were TIM2e + I + G and GTR + I + G, respectively. While clades in the *18S rRNA* tree recovered the higher phylogenetic support, neither resulted in a fully resolved phylogeny.

The tree derived from the concatenated dataset, partitioned into five blocks, resulted in mostly well-supported clades, although some relationships remained unsolved. Bayesian results showed a good convergence and thorough sampling (ASDSF < 0.005, PSRF $= 1.000 \pm 0.001$, ESS > 4000 for each parameter). Based on the phylogeny, we recognize eight main clades (A–H) and eight subclades (Fig. 3). The definition of these clades was made to match the current taxonomic treatment and the presence of distinct morphological features as far as possible (see Discussion). Support values in Fig. 3 consist of FBP and BPP. When both estimators reported non-concordant results, i.e., one supported the clade while the other did not, we also provide SH-aLRT

and TBE. Otherwise, when FBP and BPP did not support a clade, neither did SH-aLRT and TBE. All clades and subclades recognized in Fig. 3 received phylogenetic support unless otherwise stated (see below). All representative taxa of the orders Reticulariales and Liceales (outgroup) clustered into two clades, A and B, respectively. Remarkably, two species always regarded in Trichiales, *Dianema depressum* and *D. subretisporum*, branched within clade A. The remaining clades (C—H) comprised what we consider the order Trichiales s.str.

Within Trichiales, the primary distinction was between clades C–D and clades E–H. Clade C corresponded to the genus *Dictydiaethalium*, and clade D encompassed the genera *Dianema*, *Calomyxa*, *Prototrichia*, plus the species *Licea variabilis*. Clade E, in turn, split into subclades E1 and E2, and it included some *Arcyria*, *Hemitrichia*, and *Trichia* species. While subclade E2 (*Hemitrichia* and *Trichia*) received phylogenetic support, the distinct support assessment methods disagreed concerning the *Arcyria* subclade E1 (BPP = 0.99 and TBE = 0.82 versus SH-aLRT = 76.3 and FBP = 55). The bulk of *Arcyria* taxa plus *Arcyodes incarnata* and *Calonema foliicola* constituted the clade F, further divided into subclades F1 and F2. Clade G comprised three *Perichaena* species, not closely related to the two other clusters with *Perichaena* taxa (subclades H2 and H4).

Three of the four support measurements gave clade H support (SH-aLRT = 96.3, BPP = 1.0, and TBE = 0.96 versus FBP = 63), in turn, split into four subclades (H1–H4) plus some taxa with uncertain phylogenetic affinities (OT, Orphan taxa). Subclade H1 consisted of some *Hemitrichia*, *Trichia*, and *Oligonema* species. Again, support measurements did not agree for this subclade (SH-aLRT = 82.2, BPP = 0.98, and TBE = 0.92 versus FBP = 41). Subclade H2 exclusively encompassed some *Perichaena* species. A distinct subclade (H3) grouped some *Hemitrichia* and *Trichia* taxa with all *Metatrichia* species studied, although not all support measurements agreed (BPP = 0.98 and TBE = 0.97 versus FBP = 69 and SH-aLRT = 52.4). Subclade H4 comprised the bulk of *Perichaena* species plus *Trichia agaves*. Last, species *Cornuvia serpula*, *Hemitrichia crassifila*, and *Trichia varia* remained as orphan taxa (OT) within clade H. The phylogenetic relationships among these subclades remained unsolved.

The only-*18S rRNA*-based phylogeny with the expanded dataset (Supplementary material 3) showed that the specimens of each species clustered in monophyletic clades, except for *Reticularia jurana*, *Dictydiaethalium plumbeum*, *Calomyxa metallica*, *Arcyria cinerea*, *Perichaena vermicularis*, *Perichaena depressa*, *Perichaena quadrata*, and one highly divergent sequence of *Trichia favoginea*. While some specimens of each of these species did not constitute sister taxa– and more probably represent distinct species– they clustered, as closely related taxa, in the same principal clades (A–H), pointing out the stability of the morphological characters of clades A–H.

3.2. Occurrence and character evolution of the fruiting bodies features

Sporophores. Compound sporophores, i.e., aethalia and pseudoaethalia, were the less common fruiting bodies, only present in clades A (outgroup) and C (*Dictydiaethalium*). On the contrary, sporocarps, either sessile or stalked, and plasmodiocarps co-occurred in most remaining clades (Fig. 3). Only clade B comprised species producing exclusively sessile sporocarps, and sporophores of all species in E1 and F1 consisted of stalked sporocarps. Plasmodiocarps were the only sporophore type in H2.

Stalks. Ancestral state reconstructions detected different origins of the stalks in Trichiales, including clade F (*Arcyria*), a subgroup of species in H3 (*Metatrichia* and related species), and multiple individual species (Fig. 4A). *Trichia varia* (orphan taxa) can sometimes develop a stalk (not reflected in Figs. 3, 4A), which could constitute an additional origin of this structure. It remained unsolved whether stalks originated once or more in E. Stalks filled with spore-like bodies occurred in clades E and F. When including the clades C and D in the analysis and treating the character states as missing data, the ancestral state reconstructions detected the same probability for either one or two origins of spore-like bodies (results not shown). However, when excluded (since this character is not evaluable in them), the analysis described a single origin of spore-like bodies (Fig. 4B).

Capillitium. The different capillitium features studied did not define monophyletic groups (Fig. 3). According to the ultrastructural capillitium types defined in García-Cunchillos et al. (2021a), all the species known to develop solid capillitium filaments (ultrastructural capillitium type A) branched within the clades A and D. The hollow capillitium types (ultrastructural types B–E) appeared in the phylogeny as follows (see Supplementary material 7): type B, in clades E, F, and H4; type C, in subclades H1 and H3, plus the species *Trichia varia* (OT); type D, in clade G; and type E, in subclade H4. Spiral ornamentation occurred in every species in subclades E2, H1, and H3, and some species in clades D, F1, and H4 acquired this ornamentation independently. All the clades encompassed different capillitium ornamentation, even though we simplified it in the Fig. 3 iconography for practical purposes. Ramification patterns were also highly variable, and most clades and subclades included species with both network and sparsely branching architectures. Capilllitium consisting of tubules with both free ends occurred, not exclusively, in subclades E2, H1, H4, and *T. varia* (OT).

Peridium. The number of layers of the peridium was also variable among and within clades (Fig. 3). Ancestral state reconstructions inferred a single-layered peridium in the last common ancestor to Trichiales, and multiple acquisitions of a second layer occurred independently (Fig. 4C). Within clades D and H1, each common ancestor most probably developed single-layered peridia, and the acquisitions of a second layer were punctual in certain species. On the contrary, each ancestor in subclades H2, H3, and H4 developed two-layered peridia, and only some species in H2 and H4 lost the second layer. These results are uncertain concerning clade G.

Spores. Smooth spores were the least represented type, occurring in only two species in clade B. All clade A species have simple reticulate spores (muri elements); however, in Trichiales, only a group of subclade E2 species develop this ornamentation (Fig. 3). On the contrary, verrucate (verrucae) and baculate (bacula) spores were the most common types and, most probably, emerged more than once in evolutionary history (Fig. 4D). Last, cristate (cristae), encompassing the subtypes cristate reticulate and cristate patched, and pilate (pila) spores occurred in subclades H1 and H3, respectively. Besides, both ornamentations are also present in two orphan taxa (*Cornuvia serpula* and *Trichia varia*), pointing out different possible origins of these elements.

4. Discussion

4.1. Character evolution in the fruiting bodies features

Based on the new Trichiales phylogeny, the mapping of characters and the ancestral state reconstructions described intricate evolutionary patterns. The occurrence of stalks does not reflect phylogenetic relationships in Trichiales. Fiore-Donno et al. (2012) reported similar results in Stemonitidales within the dark-spored Myxomycetes. Indeed, multiple stalk losses (and subsequent acquisitions) seem to be the general pattern in Myxomycetes (Leontyev et al. 2019), unlike in other fruiting body-forming amoebozoans in which stalk loss events are unusual (Olive 1975). Similarly, multiple convergences were detected when considering the shape of the test (hard shell) in Arcellinida, another morphologically diverse amoebozoan lineage, in which the outline of this test seems to be more related to ecological conditions than to a particular evolutionary origin (González-Miguéns et al. 2022). Similar results emerged when studying the component material of the test in different groups within Arcellinida (Kosakyan et al. 2016). However, the development of stalks, at least in Trichiales, does not seem to be related to specific ecological and environmental conditions.

On the contrary, the stalk reinforcement, either with spore-like bodies or refuse matter, showed a more straightforward pattern of character evolution. Ancestral state reconstructions detected an early origin of spore-like bodies, most probably in a common ancestor to

clades E–H (*Arcyria*, *Arcyodes*, and some *Trichia* and *Hemitrichia* species). The ability to produce these bodies seems to have been subsequently lost (Fig. 4B) in clades G–H. In the latter, refuse matter fills the stalks (Martin and Alexopoulos 1969). Nonetheless, these refuse materials can differ among species (Estrada-Torres et al. 2009), and they may not be necessarily homologous, which agrees with the multiple origins of stalks in G–H (Fig. 4A).

Our phylogeny described complex evolutionary histories of the capillitium features (Fig. 3), as previous studies pointed out (Fiore-Donno et al. 2013; Leontyev et al. 2019). While spiral ornamentation was known to have originated in several clades, here we show that this acquisition occurred even in some species within clades in which the remaining species lack spirals (e.g., *Hemitrichia leiocarpa* in subclade F1). On the other hand, the loss of the capillitium, already known in *Licea variabilis* (Fiore-Donno et al. 2013) and also shown here in *Perichaena nigra* (Lado et al. 2014), or its reduction to a rudimentary capillitium (*P. liceoides*, Gilert 1990) points out that the absence of this structure does not necessarily exclude a taxon from Trichiales. See next section and Supplementary material 7 for further discussion.

The multiple origins of a second peridial layer seem to reflect convergence processes, rather than homology, which are also noticeable by their different features (compare Fig. 3G, H3, H4 and see Lado and Pando (1997) for descriptions of the peridium in Trichiales). Moreover, Mims and Rogers (1975) pointed out inconsistencies in the definition of peridium with ultrastructural and developmental approaches. This structure is the least studied in Myxomycetes, and future studies will shed light on its true nature considering morphological, developmental, and evolutionary aspects.

Two spore ornamental elements appeared early in Trichiales diversification: bacula (Fig. 2B) and verrucae (Fig. 2C). However, ancestral state reconstructions could not determine the exact evolutionary histories (Fig. 4D), and we can then consider at least two scenarios. First, a transition from baculate to verrucate ornamentation could have occurred in a common ancestor to clades E–H (Arcyriaceae and Trichiaceae). In this scenario, verrucae in E and F would be homologous elements. A subsequent transition from verrucate to baculate, with bacula (Fig. 2E) identical to those in clades C and D, should have happened in an ancestor of clades G–H. Remarkably, ornamentation in *Calonema foliicola* (clade E, Fig. 2D) was described as deviant bacula elements (García-Cunchillos et al. 2021b), although they seem to constitute a punctual verrucae modification according to our phylogeny. In the second scenario, the character state in the ancestor of clades E–H would have remained baculate, and verrucae in clades E and F would not be homologous.

Seemingly, pila (Fig. 2F) and cristae elements (Fig. 2G, H) originated from bacula in clade H (Fig. 4D). These results agree with the hypothesis proposed by Rammeloo (1974), who considered the cristae as derived elements from joint bacula. See subclade H1 in the next section for further discussion concerning the two cristate subtypes. Similarly, muri elements (Fig. 2A) seem to constitute derived forms of connected verrucae.

Accordingly, the last common ancestor to Trichiales could have produced sessile sporophores, thus without spore-like bodies, single-layered peridia, and, most probably, baculate spores. However, we should carefully consider these conclusions; many species still lack phylogenetic information, especially in the understudied genus *Licea*. Another interesting taxon to unravel the evolutionary history of the order is the monospecific genus *Trichioides* (Novozhilov et al. 2015), with smooth spores lacking ornamentation, like many *Licea* species (clade B), but developing capillitium threads twisting themselves similar to that in *Prototrichia* (clade D).

4.2. Principal clades in the Trichiales phylogeny

Despite the evolutionary patterns above described, most transitions between character states occurred within clades and subclades, and single features do not define monophyletic groups. Here, we analyze the distinctive morphological traits occurring in each clade.

4.2.1. Clades A and B

Our phylogeny recovered the orders Reticulariales and Liceales into two clades (A and B), with Liceales more closely related to Trichiales, as previous studies did (Fiore-Donno et al. 2013; Leontyev et al. 2019). Leontyev et al. (2014b) stated that the definition of pseudocapillitium may not apply to every Reticulariales taxa and proposed a true capillitium in the genera *Lycogala*, *Reticularia*, and *Alwisia*. The two *Dianema* species branching within clade A in our phylogeny (*D. depressum* and *D. subretisporum*) supports this hypothesis; TEM reports demonstrated an ultrastructural capillitium type A (García-Cunchillos et al. 2021a) in *D. depressum*. However, SEM reports showed hollow filaments in *Alwisia* (Leontyev et al. 2014b; Nelson et al. 1982) and *Lycogala* (Gaither 1976), yet TEM studies are still necessary to corroborate it.

Despite the noticeable differences (Fig. 3), all clade A species show the same simple reticulate spore ornamentation (muri elements like those depicted in Fig. 2A). Moreover, every reticulate-spored species in these and related genera (e.g., *Alwisia*, see Leontyev et al. 2014a) constituted a single clade, unlike those with other ornamentation, more closely related to the order Cribrariales (*sensu* Leontyev et al. 2019), not studied here (Leontyev et al. 2015). In *Dianema*, besides the two referred species, only *D. aggregatum* has the same simple reticulate ornamentation (Moreno et al. 2004), suggesting a close relationship with clade A, but we could not obtain genetic information (Supplementary material 2).

Clade B in our phylogeny corresponds to clade "Liceidae" in Fiore-Donno et al. (2013), order Liceales according to Leontyev et al. (2019). The genus *Licea* encompasses species lacking capillitium and pseudocapillitum, and most authors consider it an unnatural group (Eliasson 1977; Gilert 1987; Lado and Eliasson 2022). Remarkably, other clades (D, H3) also included capillitium-lacking species. Moreover, the very similar genus *Listerella* can be interpreted as a *Licea* developing capillitium or related to the genus *Perichaena*, as Eliasson (2017) suggested. Unfortunately, we could not generate DNA data from most specimens of these genera (Supplementary material 2).

4.2.2. Clade C

Clade C corresponded to the genus *Dictydiaethalium* and corroborated its branching within Trichiales, as recovered in previous studies (Fiore-Donno et al. 2013; Leontyev et al. 2019). Thus, this is the only clade in Trichiales with pseudocapillitium, better fitting the traditional definition of peridial remnants. Our results reported a close relationship between clades C and D. Remarkably, all species in these clades present the same baculate spore ornamentation (Fig. 2B), yet it also occurs in other clades (Fig. 3). Exceptionally, bacula in *D. dictyosporum* joint in short rows, although the individual bacula are still recognizable (Lado et al. 2018).

4.2.3. Clade D

Previous studies recovered close affinities among the genera *Calomyxa*, *Dianema*, and *Prototrichia* (Fiore-Donno et al. 2013; Ronikier et al. 2020); however, a broader *Dianema* taxa sampling demonstrated no such circumscriptions as different genera (Fig. 3). All species known to develop an ultrastructural capillitium type A as defined in García-Cunchillos et al. (2021a) (absent as an exception in *Licea variabilis*), i.e., nearly solid filaments, branched in this clade (Supplementary material 7) except *D. depressum*, previously mentioned (see clade A). The chief character distinguishing these genera is the capillitium ornamentation, consisting of verrucae spirally arranged in *Calomyxa* (Poulain et al. 2011), smooth threads or with occasional verrucae-like elements in *Dianema*, abundant in *D. succulenticola* (Lado et al. 2013), and with the capillitium twisting in *Prototrichia* and acquiring spiral-like structure (Lado and Pando 1997). According to our phylogeny, none of these elements correlate with phylogenetic relationships. Specimens labeled

Dianema sp. highly resemble *D. corticatum*, the only studied taxa with clustered spores, pointing out the independent occurrence of spores in clusters.

4.2.4. Clade E

Clade E comprised two subclades, yet not all support measurements agreed concerning this division (see Results). Nevertheless, our phylogeny recovered confidently, for the first time, the genus *Arcyria* as paraphyletic (clades E1 and F), yet we have not found diagnostic characters distinguishing them (see comments in clade F). Despite the noticeable differences (Fig. 3), subclades E1 and E2 share the spore-like bodies filling the stalks and an ultrastructural capillitium type B (Supplementary material 7), characters also shared with clade F species.

Fiore-Donno et al. (2013) recovered a similar clade to our subclade E2, comprising some *Hemitrichia* and *Trichia* species, and proposed the spore-like bodies as the diagnostic character. However, this definition excludes the sessile species (Fig. 3). Instead, we regard to E2 the combination of spiral capillitium ornamentation, lacking secondary spines (Lado and Pando 1997), and verrucate (with single-sized verrucae) or simple reticulate spores (muri elements, Fig. 2A).

4.2.5. Clade F

Besides the already known affinities between the genera *Arcyria* and *Arcyodes* (Fiore-Donno et al. 2013), the species *Calonema foliicola* and *Hemitrichia leiocarpa* also branched within clade F, both with an ultrastructural capillitium type B (García-Cunchillos et al. 2021a), precisely as in *Arcyria* and *Arcyodes* (Supplementary material 7). Thus, the spiral capillitium ornamentation in these species, consisting of parallel, spirally arranged veins in *C. foliicola* (Estrada-Torres et al. 2003), is to be interpreted as independent origins of this ornamentation. Remarkably, Feng and Schnittler (2017) recovered a close phylogenetic relationship between *Hemitrichia imperialis* (always with spirals) and *Arcyria stipata* (sometimes with spirals), which indicates that more spiral origins may have occurred in clade F.

Species in clade F split into two subclades related to the spore color in mass: greyish (F1) and reddish (F2). Fiore-Donno et al. (2013) already identified this distinction, yet they did not find phylogenetic support. A broader taxa sampling corroborated this division, although with exceptions. The species *C. foliicola*, while having light reddish spores (Estrada-Torres et al. 2003), clustered within F1 (greyish). Moreover, other *Arcyria* species with reddish spores constituted a distinct subclade (E1). The spore color in F1 and E1 stand out in Trichiales, usually yellowish-colored (Martin and Alexopoulos 1969). However, pigments producing these colors are still understudied (Blackwell and Busard 1978; Rebhahn et al. 1999). Beyond color, spore ornamentation was considered a stable character of the genus *Arcyria* (e.g., Martin and Alexopoulos 1969; Robbrecht 1974), consisting of verrucae of two categorical sizes (Fig. 2C). Nevertheless, our phylogeny demonstrated that this ornamentation type is not diagnostic of a single monophyletic group in Trichiales but appears in both clades E1 and F.

4.2.6. Clade G

The paraphyletic origin of the genus *Perichaena* was first reported by Walker et al. (2015), based on *P. chrysosperma* and *P. pedata*. Our results recovered a clade (G) encompassing these species plus *P. calongei*. In these taxa, the capillitium ornamentation consists of spine-like elements (Lado et al. 2009), differentiating them from the rest species in the genus. Remarkably, *P. chrysosperma* is the only known species with an ultrastructural capillitium type D (García-Cunchillos et al. 2021a), yet there is no information on the remaining species.

4.2.7. Clade H

Clade H comprised four highly diverse subclades (H1–H4) and three taxa of uncertain position or orphan taxa (OT). All species known to develop an ultrastructural capillitium type C (García-Cunchillos et al. 2021a) occurred within clade H, in H1, H3, and some orphan taxa (Supplementary material 7). Remarkably, subclade H4 was the only one that included two capillitium types. First, type B in *Perichaena corticalis*, and, second, type E, exclusively detected in *P. quadrata* (García-Cunchillos et al. 2021a). However, all other species known to have a capillitium type B branched within the clades E and F; thus, it is unknown whether capillitium type B in *P. corticalis* is vestigial of a common ancestor to clades E–H or it is the result of convergent processes. Unfortunately, ultrastructural information is lacking in subclade H2. Although phylogenetic affinities among subclades remain uncertain, a possible evolutionary hypothesis would imply type C as the ancestral state to clade H, and the other types would be modifications from it. Thus, we retain a general clade H, yet further studies are necessary to confirm its entity.

4.2.7.1. Subclade H1. Subclade H1 encompassed all the studied species with cristate spores. Only *H. intorta* and *T. alpina* showed different ornamentation (Fig. 4D). While it seems more plausible that both species diverged before the origin of the cristae elements, their phylogenetic affinities remained uncertain. Our results shed light on the differentiation between the cristate reticulate (Fig. 2G) and patched (Fig. 2H) subtypes (García-Cunchillos et al. 2021b). All species with cristate patched spores formed a monophyletic group (Fig. 3). Instead, the phylogeny did not corroborate whether the cristate reticulate subtype originated once.

Our phylogeny also recovered *Oligonema* as a paraphyletic genus, described with capillitium ornamentation consisting of faint or even lacking spirals (de Haan et al. 2004). Fiore-Donno et al. (2013) already noted this paraphyly based on *18S rRNA* sequences of *O. schweinitzii* and *O. flavidum*. Thus, several spiral losses seem to have occurred within H1. The exact affinities of specimens labeled *Oligonema* sp. will require extensive sampling.

4.2.7.2. Subclade H2. Subclade H2 encompassed the three *Perichaena* species studied that form plasmodiocarps, as previously reported by Ronikier et al. (2020). However, a broader representation of *P. vermicularis* revealed that this taxon encompasses cryptic diversity, comprising distinct non-sister species, as detected with *Calomyxa metallica* (clade D). Besides the fruiting bodies type, the capillitium ornamentation was a diagnostic character of the clade, consisting of more or less prominent and cylindrical elements (Ronikier et al. 2013, 2020).

4.2.7.3. Subclade H3. All subclade H3 species present spores ornamented with pila (Fig. 2F). But, as previously stated, we can not discard multiple origins of these elements (Fig. 4D). Notably, the genus *Metatrichia* is probably the only monophyletic genus in Trichiales as initially described. Besides, all species develop two-layered peridia yet with remarkably variable features. For instance, peridia in *Metatrichia* are coriaceous or cartilaginous (Fig. 3H3). In *H. pardina*, the peridium develops wart-like projections (Lado and Pando 1997). Thus, the second peridial layer may not be homologous even within subclade H3.

4.2.7.4. Subclade H4. Subclade H4 comprised the bulk of *Perichaena* species studied, developing sessile sporocarps, except *P. stipitata* (Fig. 3H4). Unexpectedly, the species *Trichia agaves* branched within this clade, being yet another example of independent capillitium spiral origin. Peridium dehiscence distinguishes H4 from the other clades comprising *Perichaena* species (G, H2). In most Trichiales, peridium dehiscence consists of an irregular break (Martin and Alexopoulos 1969), after which only a few peridium remnants remain in the sporophore. However, most species in H4, including *T. agaves* (Mosquera et al. 2000), show circumscissile dehiscence, i.e., a circling dehiscence line divides the sporotheca into a lid and a spore-filled base (Clark and Haskins 2014), except in *P. liceoides*, with irregular dehiscence (Poulain et al. 2011). Species *P. luteola* branched within this subclade based on *18S rRNA* sequences (results not shown), as previously detected in Fiore-

Donno et al. (2013).

4.2.7.5. Orphan taxa (OT). Within the three orphan taxa, *Trichia varia* presents pilate spores and capillitium ornamented with smooth spirals (García-Cunchillos et al., 2021b), similar to subclade H3 species. *Hemitrichia crassifila* (baculate spores, capillitium with spirals bearing cylindrical projections) highly resembles *Hemitrichia intorta*, while we did not recover such phylogenetic affinities, as pointed out in Ronikier et al. (2020). Remarkably, the species *Cornuvia serpula* shows distinctive, large discs embracing the capillitium filaments (sometimes named rings) and unique cristate reticulate-like spores (Estrada-Torres et al. 2015). While our phylogeny reported a close relationship to H2, this affinity did not receive support.

4.3. Taxonomic implications

The results of our and previous phylogenies highlight the need for a taxonomic review of the order Trichiales. Regarding the taxonomic rank of order, our results corroborated the inclusion of the genus *Dictydiaethalium* and the species *Licea variabilis* in Trichiales. Besides, according to our results, the species *Dianema subretisporum* and *D. depressum* cannot be longer circumscribed in the order (Fig. 3). However, since their exact affinities within clade A remained unsolved, and our study is not focused on taxa outside Trichiales, we do not propose any nomenclatural change.

As for the family rank, we provisionally divide the order into four families (Fig. 3). First, Dictydiaethaliaceae (clade C), with a single genus, *Dictydiaethalium*, instead of considering the genus in the family Dianemataceae (Leontyev et al. 2019), to reflect its notable differences compared to the other genera in the order (pseudoaethaloid sporophores and pseudocapillitium). Second, Dianemataceae (clade D), including the genera *Calomyxa*, *Dianema*, *Prototrichia*, and the species *Licea variabilis*. Third, Arcyriaceae *sensu lato*, including clades E1 and F, and *sensu stricto*, limited to clade F. Although this family remains in this way paraphyletic, its morphological consistency makes it worth recognizing, albeit temporarily (see below). Lastly, we retain the remaining taxa, encompassing clades G and H, in the family Trichiaceae.

Some generic boundaries within Arcyriaceae and Trichiaceae remained uncertain, so we only propose taxonomic changes, when necessary, for taxa studied here and with phylogenetic support. On the contrary, we do not propose any modifications for species either not studied here or with unsolved phylogenetic relationships. Thus, we refer to both a *sensu stricto* and *sensu lato* concept for those taxa (family Arcyriaceae, and the genera *Arcyria*, *Hemitrichia*, *Oligonema*, and *Trichia*, see below) that will require more study to ascertain their position in Trichiales phylogeny. We provide the synonyms of each family and genus, their types, basionyms of the new combinations, and MycoBank numbers. A comprehensive list of synonyms for all species analyzed is available in Lado (2005–2022). We provide morphological diagnoses only for new taxa or reinstatement of previous ones, at the genera and family ranks, or when amending or expanding an existing one. We use one, two, or three asterisks to remark taxa at the taxonomic ranks of family, genus, and species, respectively.

4.3.1. Clade C

* **Dictydiaethaliaceae** Luerss. Handb. syst. Bot. 1: 42 (1877).

Type: *Dictydiaethalium* Rostaf., Vers. Syst. Mycetozoen 5 (1873).

= Clathroptychiaceae Rostaf. ex Cooke, Contr. mycol. brit. 55 (1877).

Type: *Clathroptychium* Rostaf., Sluzowce monogr. 225 (1875).

Observations: We retain the family Dictydiaethaliaceae, transferred to Trichiales, to reflect its outstanding features within the order (pseudoaethalia as sporophores and pseudocapillitium).

** ***Dictydiaethalium*** Rostaf., Vers. Syst. Mycetozoen 5 (1873).

Type: *Reticularia plumbea* (Schumach.) Fr., Syst. mycol. 3(1): 88 (1829) [≡ *Dictydiaethalium plumbeum* (Schumach.) Rostaf., in Lister, Monogr. mycetozoa, ed. 1, 157 (1894)].

= *Clathroptychium* Rostaf., Sluzowce monogr. 225 (1875).

Type: *Clathroptychium rugulosum* (Wallr.) Rostaf., Sluzowce monogr. 225 (1875) [= *Dictydiaethalium plumbeum* (Schumach.) Rostaf., in Lister, Monogr. mycetozoa, ed. 1, 157 (1894)].

= *Ophiuridium* Hazsl., Oesterr. Bot. Z. 27: 84 (1877).

Type: *Ophiuridium dissiliens* Hazsl., Oesterr. Bot. Z. 27: 85 (1877) [= *Dictydiaethalium plumbeum* (Schumach.) Rostaf., in Lister, Monogr. mycetozoa, ed. 1, 157 (1894)].

Species included here: *D. dictyosporum* Nann.-Bremek., *D. plumbeum* (Schumach.) Rostaf.

4.3.2. Clade D

* **Dianemataceae** T. Macbr. N. Amer. Slime-moulds, ed. 1, 179 (1899), as "Dianemeae".

Type: *Dianema* Rex, Proc. Acad. Nat. Sci. Philadelphia 73: 397 (1891).

= Margaritaceae Lister, Monogr. mycetozoa, ed. 1, 202 (1894), nom. illeg. [Art. 18.3].

Type: *Margarita* Lister, Monogr. mycetozoa, ed. 1: 203 (1894), nom. illeg. [Art. 53], non *Margarita* Gaudin, Fl. Helv. 5. 335 (1829).

= Prototrichiaceae T. Macbr., N. Amer. Slime-moulds, ed. 1: 179 (1899), as "Prototrichieae".

Type: *Prototrichia* Rostaf., Sluzowce monogr. suppl.: 38 (1876).

Morphological diagnosis: The capillitium, absent in *Licea variabilis*, consists of nearly solid filaments (threads), usually attached to the apex and base of the sporotheca. Threads either smooth or with scattered verrucae or twisting themselves and acquiring a spiral-like structure.

Observations: Martin (1949) already treated the genera *Dianema*, *Calomyxa* (as "*Margarita*"), and *Prototrichia* under a single family Dianemataceae (as "Dianemaceae"), indirectly setting the priority between Dianemataceae and Prototrichiaceae. Nevertheless, in case of doubt, we are here explicitly adopting the name Dianemataceae and relegating Prototrichiaceae as a synonym. While the second edition (1922) of Macbrides's North American Slime-moulds is sometimes cited as the place of valid publication of Dianemataceae, the family was already validly published in the first edition (1899), albeit with an improper termination, which can be corrected (Art. 18.4 ICN, Turland et al. (2017)). The order names ending as families are not to be treated as families (Note 3 of Art. 18.2), which became explicit in the second edition of the monograph. As previously stated, our phylogeny does not support the circumscription of these three genera; moreover, the types of *Dianema* (*D. harveyi*) and *Prototrichia* (*P. metallica*) are very closely related, making it impossible to treat both genera separated. However, we do not propose nomenclatural changes until we comprehensively understand the morphological boundaries and the phylogenetic relationships within this highly diverse clade.

** ***Calomyxa*** Nieuwl., Amer. Midl. Naturalist 4:335 (1916) [published as nom. nov. for *Margarita* Lister].

Type: *Calomyxa metallica* (Berk.) Nieuwl., Amer. Midl. Naturalist 4: 335 (1916) [≡ *Physarum metallicum* Berk., Mag. Zool. Bot. 1: 49 (1837).

≡ *Margarita* Lister, Monogr. mycetozoa, ed. 1, 203 (1894), nom. illeg. [Art. 53], non *Margarita* Gaudin, Fl. Halv. 5. 335 (1829).

Type: *Margarita metallica* (Berk.) Lister, Monogr. mycetozoa, ed. 1, 203 (1894) [≡ *Physarum metallicum* Berk., Mag. Zool. Bot. 1: 49 (1837).

Species included here: *C. metallica* (Berk.) Nieuwl.

** ***Dianema*** Rex, Proc. Acad. Nat. Sci. Philadelphia 43: 397 (1891).

Type: *Dianema harveyi* Rex, Proc. Acad. Nat. Sci. Philadelphia 43: 397 (1891).

= *Lamprodermopsis* Meyl., Bull. Soc. Vaud. Sci. Nat. 46: 56 (1910).

Type: *Lamprodermopsis nivalis* Meyl., Bull. Soc. Vaud. Sci. Nat. 46: 56 (1910).

Species included here: *D. corticatum* Lister, *D. harveyi* Rex, *D. inconspicuum* Poulain, Mar. Mey. & Bozonnet, *D. mongolicum* Novozh., *D. nivale* (Meyl.) G. Lister, *D. succulenticola* Lado, Estrada & D. Wrigley.

** ***Prototrichia*** Rostaf., Sluzowce monogr. suppl. 38 (1876).

Type: *Prototrichia flagellifer* (Berk. & Broome) Rostaf., Sluzowce monogr. suppl. 38 (1876) [≡ *Trichia flagellifer* Berk. & Broome, Ann. Mag. Nat. Hist., ser. 3 18: 56 (1866), = *Prototrichia metallica* (Berk.) Massee, J. Roy. Microscop. Soc. London 1889(3): 350 (1889) ≡ *Trichia metallica* Berk., in hooker, Fl. Tasman. 2(9): 268 (1859)].

Species included here: *P. metallica* (Berk.) Massee.

4.3.3. Clades E and F

* **Arcyriaceae** Rostaf. ex Cooke, Contr. mycol. brit. 69 (1877) s.l.

Type: *Arcyria* F.H. Wigg., Prim. fl. holsat. 109 (1780).

Morphological diagnosis: Sporophores sporocarpic (ocasionally in densely packed groups) Stalks, normally present, filled with spore-like bodies. Capillitium consisting of hollow filaments (tubules) ornamented with cogs, rings, half-rings, reticula, ridges, spines, spirals, warts, or a combination of them. If sporophores sessile, spore ornamentation always consisting of verrucae and capillitium ornamentation either with reticula or smooth spirals.

Observations: Phylogenetic results showed a paraphyletic origin of the genus *Arcyria*, refuting the current definition of the family Arcyriaceae. However, morphological differences among the clades comprising *Arcyria* species (E1, F) were not evident. Moreover, it remains unknown which other species, apart from those studied here, belong to subclade E1. Thus, we retain a concept of the family Arcyriaceae *sensu lato* (clades E and F), but, on the contrary, if a family Arcyriaceae *sensu stricto* is to be defined, it should only include clade F. Besides, *Hemitrichia clavata*, the type of the genus *Hemitrichia*, branched within subclade E2 along with other *Hemitrichia* and *Trichia* species. Therefore, we amended the genus *Hemitrichia sensu stricto*, transferring it from the family Trichiaceae to Arcyriaceae *sensu lato* and expanding its diagnosis.

4.3.3.1. Subclades E1, F1, F2.

** ***Arcyria*** F.H. Wigg., Prim. fl. Holsat. 109 (1780) s.l.

Type: *Arcyria clathroides* F.H. Wigg., Prim. fl. holsat. 109 (1780) [= *Clathrus denudatus* L., Sp. pl. 2: 1179 (1753) ≡ *Arcyria denudata* (L.) Wettst., Verh. Zool.-Bot. Ges. Wien 35: 535 (1886)].

= *Nassula* Fr., Summa veg. Scand. 456 (1849).

Type: *Nassula globosa* (Schwein.) Fr., Summa veg. Scand. 456 (1849) [≡ *Arcyria globosa* Schwein., Schriften Naturf. Ges. Leipzig 1: 64 (1822), non *Arcyria globosa* Weinm., 1829].

= *Arcyrella* (Rostaf.) Racib., Rozpr. Spraw. Posiedzen Wydz. Mat.-Przyr. Akad. Umiejetn 12: 80 (1884).

Type (designated here; MBT10008916): *Arcyria incarnata* (Pers. ex J. F. Gmel.) Pers., Observ. mycol. 1: 58 (1796).

= *Heterotrichia* Massee, Monogr. Myxogastr. 139 (1892) [provisional synonym].

Type: *Heterotrichia gabriellae* Massee, Monogr. Myxogastr. 140 (1892) [= *Arcyria ferruginea* Saut., Flora 24: 316 (1841)].

= *Arcyodes* O.F. Cook, Science 15:651 (1902).

Type: *Arcyodes incarnata* (Alb. & Schwein.) O.F. Cook, Science 15:651 (1902) [≡ *Licea incarnata* Alb. & Schwein., Consp. fung. lusat. 109 (1805)].

Morphological diagnosis: In addition to the family characteristics, spores ornamented with verrucae of two sizes, i.e., large, scattered verrucae and small, unevenly distributed verrucae. If capillitium ornamentation consists of parallel and sub-parallel veins, then the spores ornamented with bacula.

*** ***Arcyria foliicola*** (Estrada, J.M. Ramírez & Lado) García-Cunch., J.C. Zamora & Lado, **comb. nov.**

Basionym: *Calonema foliicola* Estrada, J.M.Ramírez & Lado, Mycologia 95(2): 354 (2003).

(MycoBank MB845391).

Species included here in *Arcyria sensu stricto* (see observations): *A. affinis* Rostaf., *A. afroalpin*a Rammeloo, *A. cinerea* (Bull.) Pers., *A. congesta* (Sommerf.) Berk. & Broome (=*Arcyodes incarnata* [Alb. & Schwein.] O.F. Cook), *A. denudata* (L.) Wettst., *A. foliicola* (Estrada, J.M. Ramírez & Lado) García-Cunch., J.C. Zamora & Lado, *A. globosa* Schwein., *A. incarnata* (Pers. ex J.F. Gmel.) Pers., *A. leiocarpa* (Cooke) Massee, *A. stipata* (Schwein.) Lister.

Species included here in *Arcyria sensu lato* (in addition to those included in *Arcyria sensu stricto*): *A. ferruginea* Saut., *A. insignis* Kalchbr. & Cooke, *A. oerstedii* Rostaf.

Observations: As for the family Arcyriaceae, we consider a paraphyletic *sensu lato* (clades E1 and F) and a *sensu stricto* (clade F) concept of *Arcyria*. The apparent lack of diagnostic morphological features for distinguishing clade E1 from F precludes an appropriate resurrection of the genus *Heterotrichia*. The genus *Arcyodes*, with its single species *Arcyodes incarnata*, is included with *Arcyria* (subclade F2), but since the name *Arcyria incarnata* is occupied and represents another species (*Arcyria incarnata* [Pers. ex J.F. Gmel.] Pers., Observ. mycol. 1: 58 [1796]), we used the name of a previous synonym of *Arcyodes incarnata*, *Arcyria congesta* (Sommerf.) Berk. & Broome, Ann. Mag. Nat. Hist., ser. 4 17:140 (1876) (≡ *Physarum congestum* Sommerf., Suppl. Fl. Lapp.: 241 [1826]). We also recover the name *Arcyria leiocarpa* (Cooke) Massee, Monogr. Myxogastr. 167 (1892) (=*Hemitrichia leiocarpa* (Cooke) Lister, Monogr. mycetozoa, ed. 1, 177 (1894)). As stated in García-Cunchillos et al. (2021a), this taxon could be hiding some cryptic diversity of distinct, non-sister species. Martin (1966) intended to typify *Arcyrella* with *A. irregularis* Racib., a name not included in the protologue of the basionym, *Arcyria* subg. *Arcyrella*, and thus not eligible for typification. Martin (1966) also indicated that *Arcyrella irregularis* is equated with *Arcyria incarnata* (one of the species names originally included by Rostafinski), and then we opted to designate it as the type of *Arcyrella* to keep the concept of this generic name unchanged.

4.3.3.2. Subclade E2.

** ***Hemitrichia*** Rostaf., Vers. Syst. Mycetozoen 14 (1873).

Type: *Trichia clavata* Pers., Neues Mag. Bot. 1: 90 (1794) [≡ *Hemitrichia clavata* (Pers.) Rostaf., in Fuckel, Jahrb. Nassauischen Vereins Naturk. 27–28: 75 (1873)].

≡ *Hemiarcyria* Rostaf., Sluzowce monogr. 261 (1875).

Type: *Hemiarcyria clavata* (Pers.) Rostaf., Sluzowce monogr.: 264 (1875) [≡ *Hemitrichia clavata* (Pers.) Rostaf., in Fuckel, Jahrb. Nassauischen Vereins Naturk. 27–28: 75 (1873)].

Morphological diagnosis: In addition to the family characteristics, capillitium tubules ornamented with spirals. Spores ornamented with single-sized verrucae or joined muri elements forming simple reticulate or sub-reticulate patterns.

*** ***Hemitrichia decipiens*** (Pers.) García-Cunch., J.C. Zamora & Lado, **comb. nov.**

Basionym: *Arcyria decipiens* Pers., Ann. Bot. (Usteri) 15: 35 (1795) [≡ *Trichia decipiens* (Pers.) T. Macbr., N. Amer. Slime-moulds, ed. 1, 218 (1899)].

(MycoBank MB845392).

*** ***Hemitrichia lutescens*** (Lister) García-Cunch., J.C. Zamora & Lado, **comb. nov.**

Basionym: *Trichia contorta* var. *lutescens* Lister, Monogr. mycetozoa, ed. 1, 169 (1894) [≡ *Trichia lutescens* (Lister) Lister, J. Bot. 35:216 (1897)].

(MycoBank MB845394).

Species included here: *H. abietina* (Wigand) G. Lister, *H. calyculata* (Speg.) M.l. Farr, *H. clavata* (Pers.) Rostaf., *H. decipiens* (Pers.) García-Cunch., J.C. Zamora & Lado, *H. lutescens* (Lister) García-Cunch., J.C. Zamora & Lado.

4.3.4. Clades G and H

* **Trichiaceae** Chevall., Fl. gén. env. Paris 1:322 (1826).

Type: *Trichia* Haller, Hist. stirp. Helv. 3: 114 (1768).

= Perichaenaceae Rostaf. ex Cooke, Contr. mycol. brit. 77 (1877).

Type: *Perichaena* Fr., in Fries & Lindgren, Symb. gasteomyc., fasc. 2: 11 (1817).

Morphological diagnosis: Stalks, when present, filled with refuse matter. Spores ornamented with bacula, pila, or cristae elements, the latter forming reticulate patterns.

4.3.4.1. Clade G. ** ***Ophiotheca*** Curr., Quart. J. Microscop. Sci. 2: 241 (1854).

Type: *Ophiotheca chrysosperma* Curr., Quart. J. Microscop. Sci. 2: 241 (1854) [≡ *Perichaena chrysosperma* (Curr.) Lister, Monogr. mycetozoa, ed. 1, 196 (1894)].

Morphological diagnosis: Capillitium tubules of not uniform diameter, ornamented with long or short spines. Dehiscence irregular or fisural. Spores ornamented with bacula elements.

*** ***Ophiotheca calongei*** (Lado, D. Wrigley & Estrada) García-Cunch., J.C. Zamora & Lado, **comb. nov.**

Basionym: *Perichaena calongei* Lado, D. Wrigley & Estrada, in Lado, Wrigley, Estrada, García Carvajal, Aguilar & Hernández-Crespo, Anales Jard. Bot. Madrid 66S1: 64 (2009).

(MycoBank MB845395).

*** ***Ophiotheca pedata*** (Lister & G. Lister) García-Cunch., J.C. Zamora & Lado, **comb. nov.**

Basinonym: *Perichaena variabilis* var. *pedata* Lister & G. Lister, J. Bot. 42:139 (1904) [≡ *Perichaena pedata* (Lister & G. Lister) G. Lister ex E. Jahn, Ber. Deutsch. Bot. Ges. 36(10): 667 (1919)].

(MycoBank MB845396).

Species included here: *O. calongei* (Lado, D. Wrigley & Estrada) García-Cunch., J.C. Zamora & Lado, *O. chrysosperma* Curr., *O. pedata* (Lister & G. Lister) García-Cunch., J.C. Zamora & Lado.

Observations: We recovered the generic name *Ophiotheca*, with the type of the genus, *Ophiotheca chrysosperma* Curr., Quart. J. Microscop. Sci. 2:241 (1854) [≡ *Perichaena chrysosperma* (Curr.) Lister, Monogr. mycetozoa, ed. 1, 196 (1894)], to name the clade encompassing species with capillitium tubules of not uniform diameter, ornamented with distinct spines, and irregular or fisural peridium dehiscence.

4.3.4.2. Subclade H1. ** ***Oligonema*** Rostaf., Sluzowce monogr. 291 (1875).

Type: *Oligonema nitens* (Lib.) Rostaf., Sluzowce monogr. 291 (1875) [≡ *Oligonema schweinitzii* (Berk.) G.W. Martin, Mycologia 39(4):460 (1947)].

Morphological diagnosis: Capillitium tubules of uniform diameter, ornamented with spirals, usually bearing spines. Spores ornamented with cristae elements forming a cristate patched pattern.

*** ***Oligonema affine*** (de Bary) García-Cunch., J.C. Zamora & Lado, **comb. nov.**

Basionym: *Trichia affinis* de Bary, in Fuckel, Jahrb. Nassauischen Vereins Naturk. 23–24: 336 (1870).

(MycoBank MB845397).

*** ***Oligonema favogineum*** (Batsch) García-Cunch., J.C. Zamora & Lado, **comb. nov.**

Basionym: *Lycoperdon favogineum* Batsch, Elench. fung. continuatio prima 257 (1786) [≡ *Trichia favoginea* (Batsch) Pers., Neues Mag. Bot. 1:90 (1794)].

(MycoBank MB845398).

*** ***Oligonema persimile*** (P. Karst.) García-Cunch., J.C. Zamora & Lado, **comb. nov.**

Basionym: *Trichia persimilis* P. Karst., Not. Sällsk. Fauna Fl. Fenn. Förh 9: 353 (1868).

(MycoBank MB845399).

*** ***Oligonema verrucosum*** (Berk.) García-Cunch., J.C. Zamora & Lado, **comb. nov.**

Basionym: *Trichia verrucosa* Berk., in Hooker, Fl. Tasman. 2(9): 269 (1859).

(MycoBank MB845400).

Species included here: *O. affine* (de Bary) García-Cunch., J.C. Zamora & Lado, *O. favogineum* (Batsch) García-Cunch., J.C. Zamora & Lado, *O. persimile* (P. Karst.) García-Cunch., J.C. Zamora & Lado, *O. schweinitzii* (Berk.) G.W. Martin, *O. verrucosum* (Berk.) García-Cunch., J.C. Zamora & Lado.

Observations: The genus *Oligonema* encompasses all the species studied with cristate patched spores, forming a monophyletic group within subclade H1. Remarkably, the original conception of this genus relied on the capillitium smooth spirals, usually only detectable by SEM; however, this feature does not represent a synapomorphy for this group. On the contrary, the cristate patched spore ornamentation better reflects the phylogeny. Nevertheless, it remains unknown whether species in subclade H1 presenting cristate reticulate spores should also be circumscribed within this genus. Remarkably, the species *Hemitrichia serpula* (Scop.) Rostaf. ex Lister, despite the cristate (reticulate) spore ornamentation, presents a unique morphology, forming intricate plasmodiocarps, highly deviant from any species here accepted in *Oligonema*. One of the accepted synonyms of *H. serpula*, *Hyporhamma reticulatum* (Pers.) Corda, Icon. fung. 6:13 (1854) (≡ *Trichia reticulata* Pers., Neues Mag. Bot. 1:90 [1794]), is the type of the genus *Hyporhamma* Corda, Icon. Fung. 6: 13 (1854), a name that should be taken into account in forthcoming studies on subclade H1. Moreover, the species *Hemitrichia intorta* and *Trichia alpina*, with verrucate and baculate spores, respectively, branched within subclade H1, yet with an uncertain position. Due to this uncertainty, we only propose nomenclatural changes for the studied species with cristate patched spores.

4.3.4.3. Subclade H2. ** ***Gulielmina*** García-Cunch., J.C. Zamora & Lado, **gen. nov.**

(Mycobank MB845402).

Etymology: dedicated to the eminent specialist in myxomycetes Gulielma Lister (1860–1949).

Type: *Guilelmina vermicularis* (Schwein.) I. García-Cunchillos, J. C. Zamora & Lado (see below).

Morphological diagnosis: Sporophores plasmodiocarpics. Dehiscence irregular. Capillitium tubules of not uniform diameter, ornamented with cylindrical protuberances. Spores ornamented with bacula elements.

*** ***Gulielmina megaspora*** (A. Ronikier, Lado & D. Wrigley) García-Cunch., J.C. Zamora & Lado, **comb. nov.**

Basionym: *Perichaena megaspora* A. Ronikier, Lado & D. Wrigley, Mycologia 105(4): 939 (2013).

(MycoBank MB845403).

*** ***Gulielmina patagonica*** (A. Ronikier & Lado) García-Cunch., J.C. Zamora & Lado, **comb. nov.**

Basionym: *Perichaena patagonica* A. Ronikier & Lado, in Ronikier, García-Cunchillos, Janik & Lado, Mycologia 112(4): 766 (2020).

(MycoBank MB845404).

*** ***Gulielmina vermicularis*** (Schwein.) García-Cunch., J.C. Zamora & Lado, **comb. nov.**

Basionym: *Physarum vermiculare* Schwein., Trans. Amer. Philos. Soc., new ser. 4(2):257 (1832) [≡ *Perichaena vermicularis* (Schwein.) Rostaf., Sluzowce monogr. Suppl. 34 (1876)].

(MycoBank MB845405).

Species included here: *G. megaspora* (A. Ronikier, Lado & D. Wrigley) García-Cunch., J.C. Zamora & Lado, *G. patagonica* (A. Ronikier & Lado) García-Cunch., J.C. Zamora & Lado, *G. vermicularis* (Schwein.) García-Cunch., J.C. Zamora & Lado.

Observations: This new genus encompasses three highly similar species traditionally considered within *Perichaena*, forming long and branching plasmodiocarps. The taxon *Gulielmina vermicularis* seems to encompass distinct, non-sister species, all of them belonging to subclade H2 (Fig. 3). Until more information is available, we retain a *sensu lato* concept of this taxon.

1. Fruiting bodies closely appressed into a pseudoaethalium; sporophore walls disappearing at maturity except for the thickened strands at the angles, which persist as pseudocapillitium depending from the lids (family Dictydiaethaliaceae).....***Dictydiaethalium***

1'. Fruiting bodies not appressed, either sporocapic or plasmodiocarpic; with true capillitium inside the sporotheca, rarely without capillitium.....**2**

2. Without capillitium.....**3**

2'. With capillitium.....**4**

3. Plasmodiocarpic; dehiscence irregular.....(see ***Licea variabilis***)

3'. Sporocarpic; dehiscence circumscissile.....***Perichaena***

4. Capillitium consisting of solid threads, attached to the base of the sporotheca and usually also to the apex (if spores simple reticulate, see *Dianema depressum* and *Dianema subretisporum*, currently not in Trichiales).....***5***

4'. Capillitium consisting of hollow tubules, free or attached only to the base of the sporotheca; tubules ornamented with spines, warts, cogs, rings, half-rings, reticula, or spirals.....**7**

5. Capillitium threads twisting themselves and acquiring a spiral-like appearance.....***Prototrichia***

5'. Capillitium threads without spiral-like appearance.....**6**

6. Capillitium smooth or with scattered verrucae.....***Dianema***

6'. Capillitium with verrucae arranged in spiral.....***Calomyxa***

7. Stalks filled with spore-like bodies. If sessile, capillitium tubules with smooth spirals or reticula and spores verrucate, simple reticulate or sub-reticulate, rarely baculate (family Arcyriaceae s.l.).....**8**

7'. Stalks not filled with spore-like bodies, usually filled with refuse matter. If sessile, capillitium tubules smooth or ornamented with ring-like elements, spines, or spirals usually bearing spines; if smooth spirals, then spore ornamentation not verrucate (family Trichiaceae).....**9**

8. Capillitium tubules ornamented with spines, warts, cogs, rings, half-rings, reticula, ridges, spirals, or a combination of them; spores ornamented with verrucae of two categorical sizes; i.e., large and small, rarely baculate.....***Arcyria***

4.3.4.4. Subclade H3. ** ***Metatrichia*** Ing, Trans. Brit. Mycol. Soc. 47 (1): 51 (1964).

Type: *Metatrichia horrida* Ing, Trans. Brit. Mycol. Soc. 47(1): 51 (1964).

Species included here: *M. floriformis* (Schwein.) Nann.-Bremek., *M. floripara* (Rammeloo) Rammeloo, *M. horrida* Ing, *M. vesparia* (Batsch) Nann.-Bremek. ex G.W. Martin & Alexop.

Observations: Subclade H3 encompassed species with pilate spores, except for *Trichia varia*, with uncertain affinities within clade H. A monophyletic group within H3 comprised all studied species circumscribed in *Metatrichia*. We consider it premature to propose any taxonomic changes until expanding the sampling of the pilate-spored species in Trichiales phylogeny.

4.3.4.5. Subclade H4. ** ***Perichaena*** Fr., in Fries & Lindgren, Symb. gasteromyc., fasc. 2: 11 (1817).

Type: *Lycoperdon corticale* Batsch, Elench. fung. 155 (1783) [≡ *Perichaena corticalis* (Batsch) Rostaf., Sluzowce monogr. 293 (1875)].

= *Pyxidium* Gray, Nat. arr. Brit. pl. 1: 580 (1821).

Type: *Pyxidium sessile* (Bull.) Gray, Nat. arr. Brit. pl. 1: 580 (1821) [= *Perichaena corticalis* (Batsch) Rostaf., Sluzowce monogr. 293 (1875)].

= *Stegasma* Corda, Icon. fung. 5: 20 (1842).

Type: *Stegasma depressum* (Lib.) Corda, Icon. fung. 5: 58 (1842) [≡ *Perichaena depressa* Lib., Pl. crypt. Arduenna 378 (1837)].

Morphological diagnosis: Sporophores sporocarpic. Peridium dehiscence typically circumscissile. Capillitium tubules of not uniform diameter. Spores ornamented with bacula elements. If dehiscence irregular, then the capillitium poorly developed, consisting of smooth, short tubules, sometimes absent.

*** ***Perichaena agaves*** (G. Moreno, Lizárraga & Illana) García-Cunch., J.C. Zamora & Lado, **comb. nov.**

Basionym: *Hemitrichia agaves* G. Moreno, Lizárraga & Illana, in Moreno, Lizárraga, Illana, Castillo & Oltra, Rivista. Micol. 43(1): 6 (2000) [≡ *Trichia agaves* (G. Moreno, Lizárraga & Illana) Mosquera, Lado, Estrada & Beltrán-Tej., in Lado, Cuad. Trab. Fl. Micol. Iber. 16: 82 (2001)].

8'. Capillitium tubules ornamented with spirals; spores ornamented with single-sized verrucae or joined muri elements forming simple reticulate or sub-reticulate patterns.....***Hemitrichia* s.str.**

9. Spores reticulate, cristate reticulate, or cristate patched.....**10**
9'. Spores baculate or pilate, rarely verrucate.....**12**

10. Capillitium tubules ornamented with prominent coarse rings.....***Cornuvia***
10'. Capillitium tubules smooth or ornamented with spirals.....**11**

11. Spores cristate patched.....***Oligonema* s.str.**
11'. Spores cristate reticulate.....**16**

12. Peridium double, cartilaginous.....***Metatrichia***
12'. Peridium single, if double not cartilaginous.....**13**

13. Dehiscence tipically circumscissile, if irregular, then capillitium reduced, consisiting of smooth tubules.....***Perichaena***
13'. Dehiscence fisural and/or irregular; capillitium well-developed and ornamented.....**14**

14. Capillitium tubules not of uniform diameter lacking spirals.....**15**
14'. Capillitium tubules of uniform diameter, ornamented with spirals.....**16**

15. Sporocarps sessile or stalked, rarely plasmodiocarps; capillitium tubules ornamented with long or short spines.....***Ophiotheca***
15'. Plasmodiocarps; capillitium tubules ornamented with cylindrical protuberances.....***Gulielmina***

16. Capillitium tubules single, with free ends.....***Trichia* s.l.**
16.' Capillitium tubules branched, forming a net, without free ends or scanty.....***Hemitrichia* s.l.**

(MycoBank MB845401).

Species included here: *P. agaves* (G. Moreno, Lizárraga & Illana) García-Cunch., J.C. Zamora & Lado, *P. corticalis* (Batsch) Rostaf., *P. depressa* Lib., *P. dictyonema* Rammeloo, *P. liceoides* Rostaf., *P. nigra* D. Wrigley, Lado & Estrada, *P. quadrata* T. Macbr., *P. stipitata* Lado, Estrada & D. Wrigley.

Observations: The genus *Perichaena sensu stricto* encompasses all the species branching within subclade H4. It includes all traditionally considered *Perichaena* species with circumscissile dehiscence plus *P. liceoides*. This genus includes one capillitium lacking species, *P. nigra*, plus the species *P. agaves*, previously considered within *Trichia*.

4.3.4.6. Orphan taxa (OT). ** ***Cornuvia*** Rostaf., Vers. Syst. Mycetozoen 15 (1873).

Type: *Cornuvia serpula* (Wigand) Rostaf., in Fuckel, Jahrb. Nassauischen Vereins Naturk. 27–28: 76 (1873).

Species included: *Cornuvia serpula* (Wigand) Rostaf.

Observations: *Cornuvia* is a monospecific genus, and we retain it to highlight its morphological and phylogenetic particularities.

** ***Trichia*** Haller, Hist. stirp. Helv. 3: 114 (1768).

Type: *Trichia ovata* Pers., Observ. mycol. 1: 61 (1796) [= *Trichia varia* (Pers. ex J.F. Gmel.) Pers., Neues Mag. Bot. 1: 90 (1794)].

=? *Trichulius* Schmidel ex Corda, Icon. fung. 5: 20 (1842).

Note: No species names were included in *Trichulius* by the authors. The identity of the name is based on Schmidel's (1782) "*Trichulius stipitatus globosus*", which illustration and description may apply to several species in Trichiales.

Species included (in a strict sense): *Trichia varia* (Pers. ex J.F. Gmel.) Pers.

Observations: Despite presenting pilate spores, the type species of the genus, *T. varia*, did not branch within subclade H3, although the phylogeny topology at this level is not supported, and we cannot discard alternative groupings. The uncertain phylogenetic position of this species precluded a more precise taxonomic classification of several taxa currently treated under *Trichia* s.l.

Hemitrichia crassifila A. Ronikier & Lado, the third orphan taxon, should be excluded from *Hemitrichia* s.str.; however, we do not propose any nomenclatural change because it is uncertain to which genus this species belongs.

Besides all these taxa, we could not obtain DNA data from the monospecific genus *Arcyriatella* Hochg. & Gottsb., or study specimens of the also monospecific *Minakatella* Nann.-Bremek. ex H. Neubert, Nowotny & K. Baumann. Thus, we temporarily retain both genera as possibly distinct, awaiting molecular data that could help to elucidate their phylogenetic relationships.

4.4. Provisional key to the genera of the order Trichiales

Our results demonstrate that none of the single genetic regions studied can provide a resolved phylogeny of Trichiales. Even if the combination of multiple regions recovered comparatively more robust

results, we should reconsider whether the *EF1A* is a worthy region to explore phylogenetic relationships in Myxomycetes. Here, we recovered concordant evolutionary histories when considering mitochondrial (*mtSSU*) and nuclear (*18S rRNA*, preferred genetic region to infer phylogenies in numerous protist lineages) genetic data. However, phylogenomic studies concerning Myxomycetes (Shchepin et al. 2021), or, at least, including them in a broader context (Kang et al. 2017), are still very incipient. Thus, phylogenomic approaches will become indispensable to determining the still uncertain evolutionary affinities among multiple taxa.

Besides, an increasing taxa sampling in our phylogeny has shown evolutionary patterns hitherto unknown for some morphological traits. However, most characters do not define monophyletic groups, and transitions between character states occurred within clades rather than between clades. Ancestral state reconstructions suggested the need to re-evaluate some characters and their presumed homology, such as the stalks and their different filling refuse materials in clades G–H or the distinct second peridium layers. Ultrastructural and developmental studies considering Trichiales evolutionary history and morphogenesis of the fruiting bodies will shed light on these emerging questions. The intricate evolutionary scenario hinders the proposal of a complete Trichiales systematics since some relationships remained unsolved, and we still lack phylogenetic information of multiple species. Nevertheless, our phylogeny and revised and updated classification provides a backbone in Trichiales systematics, which serve as a baseline for future studies, and contributes, with a new and broader approach, to the knowledge of the relationships among the species of this lineage in Amoebozoa.

Declaration of Competing Interest

The authors declare that they have no known competing financial interests or personal relationships that could have appeared to influence the work reported in this paper.

Acknowledgments

We thank Emilio Cano for his invaluable help in the tasks of the molecular systematics laboratory and Yolanda Ruiz-León for her technical support with scanning electron microscopy. We are sincerely grateful to Carlos de Mier for his indispensable assistance with the image processing and Joaquina María García-Martín for her counseling in the methodological aspects of the study. We appreciate the valuable commnets of Enrique Lara, Raquel Pino-Bodas, Pedro Jiménez-Mejías, Rubén González-Miguéns, and two anonymous reviewers. We also thank the assistance of the staff from the different herbaria: Claes Persson (University of Gothenburg), Dagmar Triebel (Staatliche Naturwissenschaftliche Sammlungen Bayerns), Lisa Castlebury (U.S. National Fungus Collections), and Margarita Dueñas (Real Jardín Botánico, CSIC). Besides, we would like to thank Arturo Estrada-Torres, Diana Wrigley de Basanta, Italo F. Treviño-Zevallos, Marianne Meyer, and Uno Eliasson for their help in obtaining some of the samples. The first author thanks Uppsala University for the support to visit both the Department of Organismal Biology and the Museum of Evolution.

Funding

This research was supported by the Spanish Government throughout a PhD grant (BES-2015-072763) awarded to the first author, and the Myxotropic Project (grant PGC2018-094660-B-I00, MCIN/AEI/10.13039/501100011033/, and "ERDF A way of making Europe").

Appendix A. Supplementary data

Supplementary data to this article can be found online at https://doi.org/10.1016/j.ympev.2022.107609.

References

Adl, S.M., Bass, D., Lane, C.E., Lukeš, J., Schoch, C.L., Smirnov, A., Agatha, S., Berney, C., Brown, M.W., Burki, F., Cárdenas, P., Čepička, I., Chistyakova, L., Campo, J., Dunthorn, M., Edvardsen, B., Eglit, Y., Guillou, L., Hampl, V., Heiss, A.A., Hoppenrath, M., James, T.Y., Karnkowska, A., Karpov, S., Kim, E., Kolisko, M., Kudryavtsev, A., Lahr, D.J.G., Lara, E., Le Gall, L., Lynn, D.H., Mann, D.G., Massana, R., Mitchell, E.A.D., Morrow, C., Park, J.S., Pawlowski, J.W., Powell, M.J., Richter, D.J., Rueckert, S., Shadwick, L., Shimano, S., Spiegel, F.W., Torruella, G., Youssef, N., Zlatogursky, V., Zhang, Q., 2019. Revisions to the classification, nomenclature, and diversity of Eukaryotes. J. Eukaryot. Microbiol. 66, 4–119. https://doi.org/10.1111/jeu.12691.

Altekar, G., Dwarkadas, S., Huelsenbeck, J.P., Ronquist, F., 2004. Parallel Metropolis coupled Markov chain Monte Carlo for Bayesian phylogenetic inference. Bioinformatics 20, 407–415. https://doi.org/10.1093/bioinformatics/btg427.

Anisimova, M., Gil, M., Dufayard, J.F., Dessimoz, C., Gascuel, O., 2011. Survey of branch support methods demonstrates accuracy, power, and robustness of fast likelihood-based approximation schemes. Syst. Biol. 60, 685–699. https://doi.org/10.1093/sysbio/syr041.

Blackwell, M., Busard, A., 1978. The use of pigments as a taxonomic character to distinguish species of Trichiaceae (Myxomycetes). Mycotaxon 7, 61–67.

Bollback, J.P., 2006. SIMMAP: Stochastic character mapping of discrete traits on phylogenies. BMC Bioinf. 7, 88. https://doi.org/10.1186/1471-2105-7-88.

Chernomor, O., von Haeseler, A., Minh, B.Q., 2016. Terrace aware data structure for phylogenomic inference from supermatrices. Syst. Biol. 65, 997–1008. https://doi.org/10.1093/sysbio/syw037.

Clark, J., Haskins, E., 2014. Sporophore morphology and development in the myxomycetes: a review. Mycosphere 5, 153–170. https://doi.org/10.5943/mycosphere/5/1/7.

Cusimano, N., Renner, S.S., 2014. Ultrametric trees or phylograms for ancestral state reconstruction: Does it matter? Taxon 63, 721–726. https://doi.org/10.12705/634.14.

de Haan, M., De Pauw, S., Bogaerts, A., 2004. A study of the genus *Oligonema* (Myxomycota) in Belgium. Syst Geogr Pl 74, 251–260.

Eliasson, U., 1977. Recent advances in the taxonomy of Myxomycetes. Botanical Notes 130, 483–492.

Eliasson, U., 2017. Review and remarks on current generic delimitations in the myxomycetes, with special emphasis on *Licea*, *Listerella* and *Perichaena*. Nova Hedwigia 104 (1–3), 343–350. https://doi.org/10.1127/nova_hedwigia/2015/0283.

Ellis, T.T., Scheetz, R.W., Alexopoulos, C.J., 1973. Ultrastructural observations on capillitial types in the Trichiales (Myxomycetes). T Am Microsc Soc 92, 65–79. https://doi.org/10.2307/3225172.

Estrada-Torres, A., Ramirez-Ortega, J.M., Lado, C., 2003. *Calonema foliicola* a new Myxomycete from Mexico. Mycologia 95, 354–359. https://doi.org/10.2307/3762047.

Estrada-Torres, A., Wrigley de Basanta, D., Conde, E., Lado, C., 2009. Myxomycetes associated with dryland ecosystems of the Tehuacán-Cuicatlán Valley Biosphere Reserve, Mexico. Fungal Divers 36, 17–56.

Estrada-Torres, A., Wrigley de Basanta, D., Lado, C., Rodríguez-Palma, M.M., 2015. *Cornuvia* (Myxomycetes: Trichiales), a new genus for Mexico. Rev Mex Biodivers 86, 9–13. https://doi.org/10.7550/rmb.47025.

Feng, Y., Schnittler, M., 2017. Molecular or morphological species? Myxomycete diversity in a deciduous forest in northeastern Germany. Nova Hedwigia 104 (1–3), 359–380. https://doi.org/10.1127/nova_hedwigia/2016/0326.

Fiore-Donno, A.M., Berney, C., Pawlowski, J., Baldauf, S.L., 2005. Higher-order phylogeny of plasmodial slime molds (Myxogastria) based on elongation factor 1-A and small subunit rRNA gene sequences. J. Eukaryot. Microbiol. 52, 201–210. https://doi.org/10.1111/j.1550-7408.2005.00032.x.

Fiore-Donno, A.M., Kamono, A., Meyer, M., Schnittler, M., Fukui, M., Cavalier-Smith, T., Salemi, M., 2012. 18S rDNA phylogeny of *Lamproderma* and allied genera (Stemonitales, Myxomycetes, Amoebozoa). PLoS ONE 7 (4), e35359. https://doi.org/10.1371/journal.pone.0035359.

Fiore-Donno, A.M., Clissmann, F., Meyer, M., Schnittler, M., Cavalier-Smith, T., Gribaldo, S., 2013. Two-gene phylogeny of bright-spored Myxomycetes (slime moulds, Superorder Lucisporidia). PLoS ONE 8 (5), e62586. https://doi.org/10.1371/journal.pone.0062586.

Fiore-Donno, A.M., Tice, A.K., Brown, M.W., 2018. A non-flagellated member of the Myxogastria and expansion of the Echinosteliida. J. Eukaryot. Microbiol. 66, 538–544. https://doi.org/10.1111/jeu.12694.

Fraser, C.M., Fleischmann, R.D., 1997. Strategies for whole microbial genome sequencing and analysis. Electrophoresis 18, 1207–1216. https://doi.org/10.1002/elps.1150180803.

Gaither, T.W., 1976. Ultrastructure of the pseudocapillitium and spores of the myxomycete *Lycogala epidendrum*. Liceales. Am J Bot 7, 569–575. https://doi.org/10.1002/j.1537-2197.1976.tb11859.x.

García-Cunchillos, I., Estébanez, B., Lado, C., 2021a. New approach to the ultrastructure of the capillitium in the order Trichiales (Myxomycetes, Amoebozoa) and its phylogenetic implications. Protist 172 (2), 125805. https://doi.org/10.1016/j.protis.2021.125805.

García-Cunchillos, I., Estébanez, B., Lado, C., 2021b. Spore ultrastructural features and significance of their diverse ornamental elements in the evolutionary history of the order Trichiales (Myxomycetes, Amoebozoa). Eur J Protistol 81, 125839. https://doi.org/10.1016/j.ejop.2021.125839.

García-Martín, J.M., Mosquera, J., Lado, C., 2018. Morphological and molecular characterization of a new succulenticolous *Physarum* (Myxomycetes, Amoebozoa)

with unique polygonal spores linked in chains. Eur J Protistol 63, 13–25. https://doi.org/10.1016/j.ejop.2017.12.004.
Gilert, E., 1987. Morphology and ultrastructure of the plasmodiocarpous species *Licea variabilis* and *L. retiformis* (Myxomycetes). Nord J Bot 7, 569–575. https://doi.org/10.1111/j.1756-1051.1987.tb02024.x.
Gilert, E., 1990. On the identity of *Perichaena liceoides* (Myxomycetes). Mycol. Res. 94, 698–704. https://doi.org/10.1016/S0953-7562(09)80671-0.
González-Miguéns, R., Soler-Zamora, C., Villar-DePablo, M., Todorov, M., Lara, E., 2022. Multiple convergences in the evolutionary history of the testate amoeba family Arcellidae (Amoebozoa: Arcellinida: Sphaerothecina): when the ecology rules the morphology. Zool J Linn Soc-Lond 194, 1044–1071. https://doi.org/10.1093/zoolinnean/zlab074.
Guindon, S., Dufayard, J.F., Lefort, V., Anisimova, M., Hordijk, W., Gascuel, O., 2010. New algorithms and methods to estimate maximum-likelihood phylogenies: assessing the performance of PhyML 3.0. Syst. Biol. 59, 307–321. https://doi.org/10.1093/sysbio/syq010.
Huelsenbeck, J.P., Larget, B., Alfaro, M.E., 2004. Bayesian phylogenetic model selection using reversible jump Markov Chain Monte Carlo. Mol. Biol. Evol. 21, 1123–1133. https://doi.org/10.1093/molbev/msh123.
Janik, P., Lado, C., Ronikier, A., 2020. Range-wide phylogeography of a nivicolous protist *Didymium nivicola* Meyl. (Myxomycetes, Amoebozoa): striking contrasts between the northern and southern hemisphere. Protist 171 (125771). https://doi.org/10.1016/j.protis.2020.125771.
Janik, P., Szczepaniak, M., Lado, C., Ronikier, A., 2021. *Didymium pseudonivicola*: a new myxomycete from the austral Andes emerges from broad-scale morphological and molecular analyses of *D. nivicola* collections. Mycologia 113, 1327–1342. https://doi.org/10.1080/00275514.2021.1961068.
Kalyaanamoorthy, S., Minh, B.Q., Wong, T.K.F., von Haeseler, A., Jermiin, L.S., 2017. ModelFinder: fast model selection for accurate phylogenetic estimates. Nat. Methods 14, 587–589. https://doi.org/10.1038/nmeth.4285.
Kang, S., Tice, A.K., Spiegel, F.W., Silberman, J.D., Pánek, T., Čepička, I., Kostka, M., Kosakyan, A., Alcântara, D.M.C., Roger, A.J., Shadwick, L.L., Smirnov, A., Kudryavtsev, A., Lahr, D.J.G., Brown, M.W., Leitner, T., 2017. Between a pod and a hard test: the deep evolution of amoebae. Mol. Biol. Evol. 34 (9), 2258–2270. https://doi.org/10.1093/molbev/msx162.
Katoh, K., Frith, M.C., 2012. Adding unaligned sequences into an existing alignment using MAFFT and LAST. Bioinformatics 28, 3144–3146. https://doi.org/10.1093/bioinformatics/bts578.
Katoh, K., Kuma, K., Toh, H., Miyata, T., 2005. MAFFT version 5: improvement in accuracy of multiple sequence alignment. Nucleic Acids Res. 33, 511–518. https://doi.org/10.1093/nar/gki198.
Katoh, K., Rozewicki, J., Yamada, K.D., 2019. MAFFT online service: multiple sequence alignment, interactive sequence choice and visualization. Brief Bioinform 20, 1160–1166. https://doi.org/10.1093/bib/bbx108.
Keller, H.W., Aldrich, H.C., Brooks, T.E., 1973. Corticolous Myxomycetes II: notes on *Minakatella longifila* with ultrastructural evidence for its transfer to the Trichiaceae. Mycologia 65, 768–778. https://doi.org/10.1080/00275514.1973.12019492.
Keller, H.W., Everhart, S.E., Kilgore, C.M., 2022. The Myxomycetes: introduction, basic biology, life cycles, genetics, and reproduction. In: Stephenson, S.L., Rojas, C. (Eds.), Myxomycetes. Biology, Systematics, Biogeography, and Ecology, 2nd ed. Academic Press, Amsterdam, pp. 1–45 https://doi.org/10.1016/B978-0-12-824281-0.00003-8.
Kistenich, S., Timdal, E., Bendiksby, M., Ekman, S., 2018. Molecular systematics and character evolution in the lichen family Ramalinaceae (Ascomycota: Lecanorales). Taxon 67, 871–904. https://doi.org/10.12705/675.1.
Kosakyan, A., Lahr, D.J.G., Mulot, M., Meisterfeld, R., Mitchell, E.A.D., Lara, E., 2016. Phylogenetic reconstruction based on COI reshuffles the taxonomy of hyalosphenid shelled (testate) amoebae and reveals the convoluted evolution of shell plate shapes. Cladistics 32, 606–623. https://doi.org/10.1111/cla.12167.
Lado, C., 2005–2022. An on line nomenclatural information system of Eumycetozoa. https://eumycetozoa.com/data/index.php. Accessed 18 December 2021.
Lado, C., Pando, F., 1997. Flora Mycologica Iberica, Vol. 2. Myxomycetes, I. Ceratiomyxales, Echinosteliales, Liceales, Trichiales. CSIC Editorial and J. Cramer, Madrid. https://doi.org/10.1111/j.1756-1051.1998.tb01879.x.
Lado, C., Eliasson, U., 2022. Taxonomy and systematics: current knowledge and approaches on the taxonomic treatment of Myxomycetes: updated version. In: Stephenson, S.L., Rojas, C. (Eds.), Myxomycetes. Biology, Systematics, Biogeography, and Ecology, 2nd edn. Academic Press, Amsterdam, pp. 269–324. https://doi.org/10.1016/B978-0-12-824281-0.00005-1.
Lado, C., Wrigley de Basanta, D., Estrada-Torres, A., García Carvajal, E., Aguilar, M., Hernández-Crespo, J.C., 2009. Description of a new species of *Perichaena* (Myxomycetes) from arid areas of Argentina. An Jardin Bot Madrid 66, 63–70. https://doi.org/10.3989/ajbm.2229.
Lado, C., Wrigley de Basanta, D., Estrada-Torres, A., Stephenson, S.L., 2013. The biodiversity of myxomycetes in central Chile. Fungal Divers 59, 3–32. https://doi.org/10.1007/s13225-012-0159-8.
Lado, C., Wrigley de Basanta, D., Estrada-Torres, A., García-Carvajal, E., 2014. Myxomycete diversity of the Patagonian Steppe and bordering areas in Argentina. An Jardin Bot Madrid 71 (1), e006.
Lado, C., Estrada-Torres, A., Rojas Alvarado, C., 2018. New records of genera and species of myxomycetes (Amoebozoa) from the Neotropics. Check List 14, 509–518. https://doi.org/10.15560/14.3.509.
Lado, C., Treviño-Zevallos, I.T., García-Martín, J.M., Wrigley de Basanta, D., 2022. *Diachea mitchellii*: a new myxomycete from high elevation forests in tropical Andes of Peru. Mycologia. https://doi.org/10.1080/00275514.2022.2072140.
Lara, E., Dumack, K., García-Martín, J.M., Kudryavtsev, A., Kosakyan, A., 2020. Amoeboid protist systematics: a report on the "Systematics of amoeboid protists" symposium at the VIIIth ECOP/ISOP meeting in Rome, 2019. Eur J Protistol 76, 125727. https://doi.org/10.1016/j.ejop.2020.125727.
Lemoine, F., Domelevo Entfellner, J.B., Wilkinson, E., Correia, D., Dávila Felipe, M., De Oliveira, T., Gascuel, O., 2018. Renewing Felsenstein's phylogenetic bootstrap in the era of big data. Nature 556, 452–456. https://doi.org/10.1038/s41586-018-0043-0.
Leontyev, D.V., Schnittler, M., Moreno, G., Stephenson, S.L., Mitchell, D.W., Rojas, C., 2014a. The genus *Alwisia* (Myxomycetes) revalidated, with two species new to science. Mycologia 106, 936–948. https://doi.org/10.3852/13-314.
Leontyev, D.V., Schnittler, M., Stephenson, S.L., 2014b. Pseudocapillitium or true capillitium? A study of capillitial structures in *Alwisia bombarda* (Myxomycetes). Nova Hedwigia 99 (3-4), 441–451. https://doi.org/10.1127/0029-5035/2014/0209.
Leontyev, D.V., Schnittler, M., Stephenson, S.L., 2015. A critical revision of the *Tubifera ferruginosa* complex. Mycologia 107, 959–985. https://doi.org/10.3852/14-271.
Leontyev, D.V., Schnittler, M., Stephenson, S.L., Novozhilov, Y.K., Shchepin, O.N., 2019. Towards a phylogenetic classification of the Myxomycetes. Phytotaxa 399, 209. https://doi.org/10.11646/phytotaxa.399.3.5.
Lister A (1925) A monograph of the Mycetozoa being a descriptive catalogue of the species in the herbarium of the British Museum. By Arthur Lister, F.L.S. Third edition, revised by Gulielma Lister F.L.S. with two hundred and twenty-three plates and fifty-six woodcuts, 3rd edn. The British Museum, London.
Litsios, G., Salamin, N., 2012. Effects of phylogenetic signal on ancestral state reconstruction. Syst. Biol. 61, 533–538. https://doi.org/10.1093/sysbio/syr124.
Martin, G.W., 1949. North American Flora 1, part 1 (Myxomycetes). The New York Botanical Garden, New York.
Martin, G.W., 1966. The genera of Myxomycetes. Stud Nat Hist Iowa Univ 20, 3–32.
Martin, G.W., Alexopoulos, C.J., 1969. The Myxomycetes. University of Iowa Press, Iowa City.
Mims, C.W., Rogers, M.A., 1975. A light and electron microscopic study of stalk formation in the Myxomycete *Arcyria cinerea*. Mycologia 67, 638–649. https://doi.org/10.1080/00275514.1975.12019786.
Moreno, G., Singer, H., Illana, C., 2004. A taxonomic review on the nivicolous myxomycete species described by Kowalski. II. Physarales and Trichiales. Österr Z Pilzk 13, 61–74.
Mosquera, J., Lado, C., Estrada-Torres, A., Beltrán Tejera, E., 2000. *Trichia perichaneoides*, a new Myxomycete associated with decaying succulent plants. Mycotaxon 75, 319–328.
Nannenga-Bremekamp, N.E., 1991. A guide to temperate Myxomycetes. Biopress, Bristol.
Nelson, R.K., Scheetz, R.W., Alexopoulos, C.J., 1982. Taxonomic studies in the Myxomycetes. V. Significance of peridial and spore ornamentations in the genus *Tubifera*, with a revised key to the species. Mycologia 74, 541–548. https://doi.org/10.1080/00275514.1982.12021548.
Nguyen, L.T., Schmidt, H.A., von Haeseler, A., Minh, B.Q., 2015. IQ-TREE: A fast and effective stochastic algorithm for estimating maximum-likelihood phylogenies. Mol. Biol. Evol. 32, 268–274. https://doi.org/10.1093/molbev/msu300.
Novozhilov, Y.K., van Hooff, H., Jagers, M., 2015. *Trichioides iridescens*, a new genus and new species (incertae sedis in Myxomycetes). Mycol Prog 14, 1018. https://doi.org/10.1007/s11557-014-1018-7.
Olive, S.L., 1975. The mycetozoans. Academic Press, New York.
Paradis, E., 2013. Molecular dating of phylogenies by likelihood methods: a comparison of models and a new information criterion. Mol. Phylogenet. Evol. 67, 436–444. https://doi.org/10.1016/j.ympev.2013.02.008.
Paradis, E., Schliep, K., 2019. ape 5.0: an environment for modern phylogenetics and evolutionary analyses in R. Bioinformatics 35 (3), 526–528. https://doi.org/10.1093/bioinformatics/bty633.
Poulain, M., Meyer, M., Bozonnet, J., 2011. Les Myxomycètes. Fédération mycologique et botanique Dauphiné-Savoie, Sévrier.
Rambaut, A., Drummond, A.J., Xie, D., Baele, G., Suchard, M.A., Susko, E., 2018. Posterior summarization in Bayesian phylogenetics using Tracer 1.7. Syst. Biol. 67 (5), 901–904. https://doi.org/10.1093/sysbio/syy032.
Rammeloo, J., 1974. Structure of the epispore in the Trichiaceae (Trichiales, Myxomycetes), as seen with scanning electron microscope. Bull Soc R Bot Belge 107, 353–359.
Rebhahn, M.-A., Schnittler, M., Liebermann, B., 1999. Taxonomic relevance of pigment patterns in *Arcyria* species (Trichiales, Myxomycetes) including *Arcyodes incarnata*. Nova Hedwigia 69 (3–4), 415–427. https://doi.org/10.1127/nova.hedwigia/69/1999/415.
Revell, L.J., 2012. phytools: an R package for phylogenetic comparative biology (and other things). Methods Ecol. Evol. 3, 217–223. https://doi.org/10.1111/j.2041-210X.2011.00169.x.
Robbrecht, E., 1974. The genus *Arcyria* Wiggers (Myxomycetes) in Belgium. Bull. Jard Bot. Natl. Belg. 44, 303–353. https://doi.org/10.2307/3667676.
Ronikier, A., Lado, C., 2015. Nivicolous Stemonitales from the austral Andes: analysis of morphological variability, distribution and phenology as a first step toward testing the large-scale coherence of species and biogeographical properties. Mycologia 107, 258–283. https://doi.org/10.3852/14-164.
Ronikier, A., Lado, C., Wrigley de Basanta, D., 2013. *Perichaena megaspora*, a new nivicolous species of myxomycete from the Andes. Mycologia 105, 938–944. https://doi.org/10.3852/12-191.
Ronikier, A., García-Cunchillos, I., Janik, P., Lado, C., 2020. Nivicolous Trichiales from the austral Andes: unexpected diversity including two new species. Mycologia 112, 753–780. https://doi.org/10.1080/00275514.2020.1759978.
Ronquist, F., Teslenko, M., van der Mark, P., Ayres, D.L., Darling, A., Höhna, S., Larget, B., Liu, L., Suchard, M.A., Huelsenbeck, J.P., 2012. MrBayes 3.2: Efficient Bayesian phylogenetic inference and model choice across a large model space. Syst. Biol. 61, 539–542. https://doi.org/10.1093/sysbio/sys029.

Rostafiński, J., 1874. Śluzowce (Mycetozoa) Monografia. Pamietn Towarz Nauk Sci Paryzu 5, 1–215.
Rostafiński, J., 1875. Śluzowce (Mycetozoa) Monografia. Pamietn Towarz Nauk Sci Paryzu 6, 216–432.
Rostafiński, J., 1876. Śluzowce (Mycetozoa) Monografia. Pamietn Dod. Towarz Nauk Sci 8, 1–43.
Schaap, P., Winckler, T., Nelson, M., Alvarez-Curto, E., Elgie, B., Hagiwara, H., Cavender, J., Milano-Curto, A., Rozen, D.E., Dingermann, T., Mutzel, R., Baldauf, S. L., 2006. Molecular phylogeny and evolution of morphology in the social amoebas. Science 314, 661–663. https://doi.org/10.1126/science.1130670.
Schnittler, M., Shchepin, O.N., Dagamac, N.H.A., Borg Dahl, M., Novozhilov, Y.K., 2017. Barcoding myxomycetes with molecular markers: challenges and opportunities. Nova Hedwigia 104 (1–3), 323–341. https://doi.org/10.1127/nova_hedwigia/2017/0397.
Shadwick, L.L., Spiegel, F.W., Shadwick, J.D.L., Brown, M.W., Silberman, J.D., 2009. Eumycetozoa = Amoebozoa?: SSUrDNA phylogeny of protosteloid slime molds and its significance for the Amoebozoan supergroup. PLoS ONE 4, e6754. https://doi.org/10.1371/journal.pone.0006754.
Shchepin, O., Novozhilov, Y., Woyzichovski, J., Bog, M., Prikhodko, I., Fedorova, N., Gmoshinskiy, V., Borg Dahl, M., Dagamac, N.H.A., Yajima, Y., Schnittler, M., 2021. Genetic structure of the protist Physarum albescens (Amoebozoa) revealed by multiple markers and genotyping by sequencing. Mole Ecol 31, 372–390. https://doi.org/10.1111/mec.16239.
Stephenson, S.L., Schnittler, M., Novozhilov, Y.K., 2008. Myxomycete diversity and distribution from the fossil record to the present. Biodivers. Conserv. 17, 285–301. https://doi.org/10.1007/s10531-007-9252-9.
Turland N, Wiersema J, Barrie F, Greuter W, Hawksworth D, Herendeen P, Knapp S, Kusber WH, Li DZ, Marhold K, May T, McNeill J, Monro A, Prado J, Price M, Smith G (Eds.) (2018) International Code of Nomenclature for algae, fungi, and plants (Shenzhen Code) adopted by the Nineteenth International Botanical Congress Shenzhen, China, July 2017. Regnum Vegetabile 159. Koeltz Botanical Books, Glashütten. https://doi.org/10.12705/Code.2018.
Walker, L.M., Leontyev, D.V., Stephenson, S.L., 2015. *Perichaena longipes*, a new myxomycete from the Neotropics. Mycologia 107, 1012–1022. https://doi.org/10.3852/14-330.
Wróbel, B., 2008. Statistical measures of uncertainty for branches in phylogenetic trees inferred from molecular sequences by using model-based methods. J Appl Genet 49, 49–67. https://doi.org/10.1007/BF03195249.
Zamora, J.C., Ekman, S., 2020. Phylogeny and character evolution in the *Dacrymycetes*, and systematics of *Unilacrymaceae* and *Dacryonaemataceae* fam. nov. Persoonia 44, 161–205. https://doi.org/10.3767/persoonia.2020.44.07.
Zhou, X., Shen, X.X., Hittinger, C.T., Rokas, A., 2018. Evaluating fast maximum likelihood-based phylogenetic programs using empirical phylogenomic data sets. Mol. Biol. Evol. 35, 486–503. https://doi.org/10.1093/molbev/msx302.